The wet deposition of the inorganic ions in the 320 cities across China: spatiotemporal variation, source apportionment, and dominant factors

Rui Li[a], Lulu Cui[a], Yilong Zhao[a], Ziyu Zhang[a], Tianming Sun[a], Junlin Li[a], Wenhui Zhou[a], Ya Meng[a], Kan Huang[a], Hongbo Fu[a,b,c] *

[a] *Shanghai Key Laboratory of Atmospheric Particle Pollution and Prevention, Department of Environmental Science & Engineering, Institute of Atmospheric Sciences, Fudan University, Shanghai, 200433, P.R. China*

[b] *Shanghai Institute of Pollution Control and Ecological Security, Shanghai 200092, P.R. China*

[c] *Collaborative Innovation Center of Atmospheric Environment and Equipment Technology (CICAEET), Nanjing University of Information Science and Technology, Nanjing 210044, P.R. China*

Corresponding author

fuhb@fudan.edu.cn

Abstract

The acid deposition has been considered to be a severe environmental issue in China. The pH, electrical conductivity (EC), and the concentrations of the water soluble ions (NO_3^-, Cl^-, Ca^{2+}, K^+, F^-, NH_4^+, Mg^{2+}, SO_4^{2-}, and Na^+) in the precipitation samples collected from the 320 cities during 2011-2016 across the whole China were measured. The mean concentrations of F^-, NO_3^- and SO_4^{2-} were in the order of winter (6.10, 19.44 and 45.74 μeq/L) > spring (3.45, 13.83, and 42.61 μeq/L) > autumn (2.67, 9.73, and 28.85 μeq/L) > summer (2.04, 7.66, and 19.26 μeq/L). The secondary ions (SO_4^{2-}, NO_3^- and NH_4^+), and F^- peaked in Yangtze River Delta (YRD) and Sichuan basin (SB). The

23 crustal ions (i.e., Ca^{2+}, Mg^{2+}), Na^+, and Cl^- showed the highest concentrations in the semi-arid

24 regions and the coastal cities, respectively. The statistical methods confirmed that the mean

25 anthropogenic contribution ratios to SO_4^{2-}, F^-, NO_3^-, and NH_4^+ at a national scale were 46.12%,

26 71.02%, 79.10%, and 82.40%, respectively. However, Mg^{2+} (70.51%), K^+ (77.44%), and Ca^{2+}

27 (82.17%) were mostly originated from the crustal source. Both Na^+ (70.54%) and Cl^- (60.42%) were

28 closely linked to the sea-salt aerosols. On the basis of the stepwise regression (SR) analysis, it was

29 proposed that most of the secondary ions and F^- were closely related to gross industrial production

30 (GIP), total energy consumption (TEC), vehicle ownership, and N fertilizer use, but the crustal ions

31 (Ca^{2+} and K^+) were mainly controlled by the dust events. The influence of dust days, air temperature,

32 and wind speed on ions increased from Southeast China (SEC) to Central China, and then to

33 Northwest China (NWC), whereas the influence of socioeconomic factors on acid ions (SO_4^{2-} and

34 NO_3^-) displayed the higher value in East China.

35 **Keywords:** Water-soluble ions; precipitation; spatiotemporal variation; source identification; China

36 **1. Introduction**

37   Atmospheric wet deposition generally removes efficiently the aerosol particles and dissolved

38 gaseous pollutants from the atmosphere (Garland, 1978; Al-Khashman, 2005; Migliavacca et al.,

39 2005). However, in some regions with severe air pollution, the scavenging of substantial aerosol

40 particles alters the chemical compositions of precipitation and even aggravates the acid deposition

41 (Kuang et al., 2016). Some inorganic ions (i.e., SO_4^{2-}, NO_3^-, NH_4^+, Ca^{2+}) play significant roles on

42 the terrestrial and aquatic ecosystem via wet deposition; for instance, leading to severe soil (lake)

43 acidification (alkalization), inhibiting the plant growth, and changing the regional climate (Liu et

44 al., 2011; Yan et al., 2010; Larssen and Carmichael, 2000; Larssen et al., 1999). In the past decades,

45   China has been suffered from the severe air pollution along with the population growth and

46   industrialization (Liu et al., 2016a). Therefore, the investigation of the wet deposition status of

47   inorganic ions is of great interest to the public and policy makers (Négrel et al., 2007).

48   A large amount of studies mainly focused on the spatiotemporal variation of the S and N

49   deposition around the world due to their adversely ecological effects in the past decades (Gerson et

50   al., 2016; Clemens 2006; Zhang et al., 2010). Okuda et al. (2005) showed that the SO_4^{2-}

51   concentration in the precipitation exhibited a slight decrease coupling with the decrease of the SO_2

52   concentration in Tokyo during 1990-2012. Hunová et al. (2014) reported that the averagely S

53   deposition flux decreased from 181 kg/ha/year to 100 kg/ha/year in Czech during 1995 and 2011 on

54   the basis of the data in 15 cities. Du et al. (2012) estimated that the wet deposition flux of inorganic

55   nitrogen reached 3.5 kg N/ha/year according to the average of 151 monitoring in the United States

56   during 1985-2012, which were significantly lower than that of China during the same period (11.11-

57   13.87 kg/ha/yr) (Jia et al., 2014).

58   Many researches about the S and N deposition have been extensively performed to date in China

59   in the recent years (Jia et al., 2014; Xu et al., 2015). In the past decades, the anthropogenic emissions

60   of SO_2, NO_2, and NH_3 displayed the remarkable increase along with the dramatic increase of fossil

61   fuel and fertilizer consumption in China (Jia et al., 2014; Kuribayashi et al., 2012). It was well

62   documented that the gaseous precursors containing S and N could be transformed into sulfates

63   (SO_4^{2-}), nitrates (NO_3^-), and ammonium (NH_4^+) during ageing in the atmosphere, thereby

64   contributing to the formation of airborne fine particles, of which were considered to be the main

65   reason for the persistent fog and haze pollution in China (Wang et al., 2016a; Qiao et al., 2015). At

66   a city level, Huang et al. (2008) observed that the wet deposition fluxes of SO_4^{2-}, NH_4^+, and Ca^{2+}

67   displayed the slight decrease from 1986 to 2006 in the urban of Shenzhen, whereas the wet

68   deposition of NO_3^- increased rapidly during the same period. Very recently, Pu et al. (2017) reported

69   that the SO_4^{2-} concentration in the wet deposition of Shangdianzi (a regional background station of

70   Beijing) showed slight decrease during 2003-2014, but the NO_3^- concentration showed an opposite

71   trend. At a regional scale, Pan et al. (2013) observed that the highest S wet deposition was

72   concentrated in the urban and industrial region of Tianjin among of ten sites of North China (NC).

73   Song et al. (2017) suggested that the bulk deposition fluxes were in the order of Chengdu (urban) >

74   Yanting (agricultural area) > Gongga mountain (natural reserve). At a national scale, Jia et al. (2014)

75   firstly found that the wet deposition of N in Southeast China (SEC) showed a significant decrease,

76   whereas it increased slightly in the western of China on the foundation of the data (620 monitoring

77   sites) collected from 120 cities across China during 1990 and 2010. Following this work, Liu et al.

78   (2016) further observed that the serious S deposition (79 monitoring sites) on SEC and Southwest

79   China (SWC). In these studies, the spatial distributions of both S and N were determined using the

80   spatial interpolation method, which generally required substantial monitoring sites (city > 150, and

81   monitoring site > 300). However, these conclusions were obtained based on a small quantity of

82   monitoring sites, which increased the uncertainties of the results. Meanwhile, the monitoring sites

83   in these studies were mainly located on some remote regions such as mountain or rural site rather

84   than the mixture of urban, suburban, and rural sites, which cannot accurately reflect the spatial

85   variations of inorganic ions in China. Moreover, the spatiotemporal variations of other inorganic

86   ions (i.e., K^+, Ca^+, Mg^{2+}) remained unclear to date, which were also linked to the acid deposition,

87   as well as the haze pollution in China (Mikhailova et al., 2013; Aloisi et al., 2017; Müller et al.,

88   2015).

89   Based on these field measurements, the ion levels in the deposition across China were believed

90   to be underestimated due to the few ion species measured by previous studies (Liu et al., 2016a),

91   which was closely associated with various emission sources (Kuang et al., 2016). Thus, the source

92   identification should be performed to assess accurately their contributions to the wet deposition

93   (Larssen et al., 1999). Liu et al. (2015b) identified that the Cl^- and NH_4^+ in the precipitation of Tibet

94   were both originated from the marine and crustal source using the geochemical index method. On

95   the basis of the positive matrix factorization (PMF) model, Qiao et al. (2015) showed that fossil fuel

96   combustion and agriculture were the main sources of SO_4^{2-} and NO_3^- in Jiuzhaigou (Sichuan

97   province). In a newly work reported by Leng et al. (2018), they supposed that the combustion of

98   fossil fuels, domestic sewages, and fertilizers were the main sources of the N-bearing ions on the

99   basis of the N isotope analysis. To date, some methods, including geochemical index method,

100   multivariate analyses, and isotope signatures have been utilized to identify the anthropogenic versus

101   natural sources of the inorganic ions in the precipitation. However, these methods suffered from

102   some weaknesses from different standpoints (AlKhatib and Eisenhauer 2017; Shi et al., 2014). For

103   instance, the geochemical index methods cannot estimate the contribution ratios of multiple sources

104   to Ca^{2+} and Na^+ at a spatial scale (Liu et al., 2015b). Despite the advances of multivariate analyses

105   lowering the associated uncertainties, the multi-collinearity still disturbed the predictions of these

106   models (Shi et al., 2014). The isotope signature method was costly and complex, especially for the

107   unconventional stable isotopes (i.e., K, Ca) (AlKhatib and Eisenhauer 2017), which restricted its

108   application at a large scale. Therefore, multiple source apportionment methods should be combined

109   in order to enhance the reliability of the results. Liu et al. (2015) also demonstrated that the

110   geochemical index method coupled with multiple statistics decreased the uncertainties of results.

111   Apart from the source apportionment, the key factor identification for the ions in the wet

112   deposition is also of great importance to reduce the acid deposition. At an early study, Singh and

113   Agrawal (2008) revealed that the significant increase of vehicle emissions contributed to the

114   accumulation of NO_2, which might be an important precursor of acid rain. Allen et al. (2015)

115   observed that some inland cities in arid and semi-arid regions were generally subjected to dust

116   events, which could increase the Ca^{2+} and K^+ concentrations in the wet deposition. Following this

117   work, Yu et al. (2017a) found that considerable energy consumption, gross domestic production

118   (GDP), and emitted substantial pollutants made China as major regions of acid rain around the world

119   using path analysis and correlation analysis. However, these researches only assessed the limited

120   factors for the inorganic ions in the wet deposition (Yu et al., 2016; Yu et al., 2017a), ignoring the

121   contributions of other socioeconomic and natural factors. Moreover, these researches mainly

122   focused the whole effects of the influential factors on inorganic ions at a national scale, while they

123   did not consider the spatial heterogeneity of the influential factors, resulting possibly in the great

124   deviation of the inorganic ions in the wet deposition for the different regions.

125   Here, the data of nine water-soluble ions in the precipitation including Ca^{2+}, Cl^-, F^-, K^+, Mg^{2+},

126   Na^+, NH_4^+, NO_3^-, and SO_4^{2-} in the 320 cities across the whole China were collected during 2011-

127   2016 to examine the characteristics of the main water-soluble ions in the precipitation. Specifically,

128   the objectives of our study were (1) to reveal the spatiotemporal patterns of water-soluble ions in

129   the precipitation recently in China at a national scale; (2) to identify quantitatively the source of the

130   water-soluble ions in the precipitation based on the multiple statistical methods; and (3) to seek out

131   the key factors for the inorganic ions at a spatial scale. This study supplied the systematical data for

132   comprehensive understanding on the inorganic composition in the precipitation based on the long-

133 term field measurement, at a national scale (the 1282 monitoring sites distributed in the 320 cities

134 across the whole China), which was beneficial to the implementation of appropriate strategies to

135 promote environmental protection in China.

136 **2.   Materials and methods**

137 2.1 Site description

138   The spatial distribution of field stations in National Acid Deposition Monitoring Network

139 (NADMN) is illustrated in Fig. 1. The selected 1282 monitoring sites are distributed in the 320 cities

140 across 31 provinces. These cities are classified into Northeast China (NEC), NC, SEC, Northwest

141 China (NWC), and Southwest China (SWC) (Tab. S1). Both of NEC and NC show typical

142 temperature monsoon climate, while SEC presents the subtropical monsoon climate. The SWC

143 region suffers from the combined effects of subtropical monsoon climate and tropical monsoon

144 climate. NWC suffers from the temperate continental climate and displays minor rainfall amount.

145 NEC and NC are filled with temperature deciduous forest, whereas SEC is mainly occupied by the

146 subtropical evergreen forest. The subtropical evergreen forest and tropical evergreen forest spread

147 out the SWC region. The NWC is generally filled with expansive grasslands and desert. The

148 latitudes and longitudes of all of 1282 monitoring sites range from 18.25 to 50.78° N, and from 79.57

149 to 129.25° E, respectively. Annual mean rainfall ranges from 10 to 1853 mm and the annual mean

150 air temperature varies between -6.9 and 24.3 ℃. The monitoring sites were designed as a mixture

151 of urban and background sites. 850 monitoring sites are concentrated in urban region, and 432 sites

152 in suburban and rural areas are considered as the background sites.

153 2.2 Sampling and chemical analysis

154   The real-time precipitation was collected by monitors in the field stations as a routine procedure

155   of NADMN. Samples from each monitoring site were collected using wet deposition automatic

156   collectors (diameter 30 cm) installed at 1.5 m above ground level. The cover of the collection

157   instrument opened automatically without delay when the precipitation sensor was activated and

158   closed automatically when precipitation ceased and no water remained on the sensor surface. The

159   sample in each rain event was collected and these samples were collected in all of the monitoring

160   sites simultaneously. Each sample was properly collected during the precipitation event when the

161   wet-only deposition instrument was under the normal condition. After the sampling, the pH and EC

162   values of the samples were measured immediately. The sample pH was measured using a pH meter

163   (MP-6p, HACH, USA) at 20–25°C. The EC value of the precipitation samples was determined by

164   an EC meter (CyberScan, CON1500, USA). After the analysis of pH and EC, all of the samples

165   were contained in the pre-cleaned polyethylene plastic bottles at -18°C in order to prevent the

166   possible transformation by microbes. All of the plastic buckets and the polyethylene plastic bottles

167   were cleaned with deionized water for more than three times and then air-dried in clean room prior

168   to use.

169   All of the precipitation samples were used to analyze the concentrations of the water-soluble

170   ions including NO_3^-, Cl^-, Ca^{2+}, K^+, F^-, NH_4^+, Mg^{2+}, SO_4^{2-}, and Na^+. The microporous membranes

171   (0.45 μm) were employed to remove all of insoluble particulates (< 0.45μm) from the precipitation

172   samples before the analysis. The ion concentrations were determined through ion chromatography

173   (Dionex ICS-900) equipped with a conductivity detector (ASRS-ULTRA). The CS12A column and

174   AS11-HC column were applied to determine the cations and anions, respectively. Each sample was

175   measured for more than three times and the relative standard deviation was less than 5% for each

176   ion. Analysis of the blank samples once a month confirmed that the cross contamination in the

177   present research was negligible. For each ion, the analysis of simulated precipitation suggested that

178   the relative bias was lower than 10%.

179   2.3 Data calculation

180   The monthly and annual volume-weighted mean (VWM) concentrations were calculated based

181   on the concentrations of specific ions and precipitation. The monthly and annual VWM

182   concentrations were obtained as follows:

183
$$C_x = \frac{\sum_{i=1}^{n}(C_i(x) \times P_i)}{\sum_{i=1}^{n} P_i} \tag{1}$$

184   where C_x denoted the monthly and annual VWM concentration of the given ion; $C_i(x)$ was the

185   concentration of the given ion in the precipitation (μeq/L); P_i was the precipitation in individual

186   sample. The monthly and annual VWM pH values were obtained based on the corresponding VWM

187   concentrations of H^+ via Eq. (1).

188   The wet deposition flux of the given ion was calculated using the following Eq. (2)

189
$$D_w = P_t C_w / 100 \tag{2}$$

190   where D_w was the wet deposition flux of the given ion (kg N ha^{-1}); P_t was the total amount of the

191   precipitation events (mm); C_w was the VWM concentration of each ion (mg/L); and 100 was a unit

192   conversion factor.

193   In order to obtain the contributions of various alkaline species to acid neutralization in the

194   precipitation, the neutralization factor (NF) was calculated using the following Eq. (3)-(5)

195   (Kulshrestha et al., 1995):

196
$$NF_{NH_4^+} = \frac{NH_4^+}{NO_3^- + SO_4^{2-}} \tag{3}$$

197
$$NF_{Ca^{2+}} = \frac{Ca^{2+}}{NO_3^- + SO_4^{2-}} \qquad (4)$$

198
$$NF_{Mg^{2+}} = \frac{Mg^{2+}}{NO_3^- + SO_4^{2-}} \qquad (5)$$

199   2.4 Source apportionment of ionic species in wet deposition

200   The enrichment factor (EF) has been widely applied to estimate the contribution ratios of the

201   various sources to the major ions in the previous studies (Lawson and Winchester 1979; Cao et al.,

202   2009; Lu et al., 2011). In the present study, an ion EF in the precipitation relative to the ion in the

203   sea was calculated using Na as a reference element as follows:

204
$$EF_{sea} = \frac{(X / Na^+)_{precipitation}}{(X / Na^+)_{sea}} \qquad (6)$$

205   where EF_{sea} was the enrichment indicator of a given ion in the precipitation relative to the ion in the

206   sea; X was the ion in the precipitation; $(X/Na^+)_{precipitation}$ represented the ratio of components in the

207   precipitation; $(X/Na^+)_{sea}$ denoted the ratio of components in the sea (Keene et al., 1986; Turekian,

208   1968).

209   The EF value of an ion in the precipitation relative to the corresponding ion in the soil was

210   calculated following Eq. (7):

211
$$EF_{soil} = \frac{(X / Ca^{2+})_{precipitation}}{(X / Ca^{2+})_{soil}} \qquad (7)$$

212   where EF_{soil} represented the EF value of an ion in the precipitation relative to the corresponding ion

213   in the soil; X denoted an ion in the precipitation; $(X/Ca^{2+})_{precipitation}$ was the ratio of components in

214   the precipitation; $(X/Ca^{2+})_{sea}$ denoted the ratio of components in the soil (Wei et al., 1991; Wei et al.,

215   1992; Shi et al., 1996; Zhang et al., 2012; Chen et al., 1992).

216   In order to quantify the anthropogenic source versus natural one of ionic species in the

217 precipitation. The fractions of anthropogenic, marine, and crustal source contributed to the ions in

218 the precipitation were calculated as follows:

219
$$SSF = \frac{(X/Na^+)_{sea}}{(X/Na^+)_{precipitation}} \times 100\% \quad (8)$$

220
$$CF = \frac{(X/Ca^{2+})_{soil}}{(X/Ca^{2+})_{precipitation}} \times 100\% \quad (9)$$

221
$$AF = 100\% - SSF - CF \quad (10)$$

222 where SSF represented the fraction of sea salt; CF denoted the crustal contribution; and AF denoted

223 the anthropogenic fraction. SSF was recalculated as the difference between 1 and CF when SSF was

224 greater than 1; CF was recalculated as the difference between 1 and SSF when CF was higher than

225 1.

226   Factor analysis (FA) has been widely employed to determine the contribution ratios of natural

227 and anthropogenic source to ionic species in the precipitation. First of all, FA was applied to reduce

228 the dimension of original variables (measured ion concentrations in samples) and to extract a small

229 number of principal components to analyze the relationships among the observed variables. All of

230 the factors with eigenvalues over 1 were extracted based on the Kaiser-Meyer-Olkin (KMO) test

231 and the Bartlett's test of sphericity, and were rotated using the Varimax method. The FA factor scores

232 and each ion concentration were treated as independent and dependent variables, respectively. The

233 resultant regression coefficients were employed to convert the absolute factor scores and then to

234 calculate the contribution of each PC source (Luo et al., 2015).

235 2.5 The geographical weight regression (GWR) method

236   Although the relationships between the independent variables and the dependent variables could

237 be calculated using correlation analysis and multiple linear regression analysis (MLR), these

238   methods cannot show the spatial variability of regression coefficients. Thus, the GWR method was

239   applied to explore the effects of socioeconomic factors on wet deposition of inorganic ions in

240   consideration of the spatial correlation. As an indicator to reflect the impacts of socioeconomic

241   factors on inorganic ion depositions, local regression coefficients were obtained using weighted

242   least squares with the following weighting function (Brunsdon et al., 1996):

243
$$\beta(u_i, v_i) = (X^T W(u_i, v_i) X)^{-1} X^T W(u_i, v_i) Y \quad (11)$$

244   where $\beta(u_i, v_i)$ represented the local regression coefficient at city i; X was the matrix of the

245   influential factors; Y denoted the matrix of the wet deposition fluxes of the water-soluble ions; and

246    $W(u_i, v_i)$ was an n order matrix that the diagonal elements were the spatial weighting of the influential

247   factors. The spatial weight function was calculated via the exponential distance decay form:

248
$$W(u_i, v_i) = \exp(-d^2(u_i, v_i) / b^2) \quad (12)$$

249   where $d(u_i, v_i)$ represented the distance between the location i and j, and b was the kernel bandwidth.

250   2.6 Data source and statistical analysis

251   The data of GDP, gross industrial production (GIP), N fertilizer use, vehicle ownership, urban

252   green space (UGS) during 2011-2016 were collected from China City Statistical Book. Total energy

253   consumption (TEC) during the period were obtained from China Energy Statistical Yearbook, which

254   consisted of the consumption of coal, crude oil, and natural gas. The daily meteorological factors

255   including precipitation, maximum and minimum air temperature, wind speed, air pressure, relative

256   humidity (RH) during 2011-2016 were collected from China Meteorological Data Network. The

257   daily visibility data during 2011-2016 was collected from National Centers for Environmental

258   Prediction (NCEP). The data of dust days were calculated based on the horizon visibility data. The

259   days with the visibility lower than 1 km were treated as the dust days. The daily data of $PM_{2.5}$, PM_{10},

260   SO_2, and NO_2 were downloaded from the National Environmental Monitoring Platform

261   (https://www.aqistudy.cn/historydata/). These data at a national scale were open access since

262   January 2014. To match the meteorological data at a national scale, the data of air pollutants during

263   2014-2016 were applied to investigate the relationships of the water-soluble ions, meteorological

264   factors, and the air pollutants in the atmosphere (Tab. S2). In addition, the SR analysis was employed

265   to determine the key factors regulating the wet deposition fluxes of the water-soluble ions. All of

266   the statistical analysis were performed by the software package of ArcGIS 10.2, SPSS 21.0, and

267   Origin 8.0 for Windows 10.

268   **3 Results and discussion**

269   3.1 The pH and EC values in the precipitation

270   To obtain the preliminary knowledge about the precipitation characteristics, the basic

271   physiochemical properties including pH and EC of the precipitation samples are presented in Fig.

272   2. The annually pH during 2011 and 2016 ranged from 5.45 ± 0.27 (mean $\pm$ standard deviation) to

273   5.94 ± 0.46 and the mean value was 5.76 (Fig. 2a). Seinfeld (1986) estimated that the precipitation

274   with pH lower than 5.60 was considered as acid rain because the pH value of natural water in

275   equilibrium with atmospheric CO_2 was 5.60. However, the CO_2 level has been increasing in recent

276   years and thus the equilibrium pH has changed (McGlade and Ekins 2015) Therefore, the average

277   CO_2 concentration during 2011-2016 (396.83 ppm) around the world was applied to the present

278   study (http://www.ipcc.ch/). The ionization equation of CO_2 include $CO_2+H_2O=H_2CO_3$ and

279    $H_2CO_3=HCO_3^-+H^+$. The dissociation constant of two equations are 3.47×10^{-2} (K_0) and 4.4×10^{-7} (K_1),

280   respectively. The $(c(H+))^2 = K_0 \times K_1 \times P_{CO2} = 6.06 \times 10^{-12}$. Therefore, the equilibrium pH was 5.61,

281   which was slightly higher than the current value (pH = 5.60). Herein, 41% of the samples during

282   the measurement showed the pH value below 5.61. Compared with the pH value of the precipitation

283   during 1980-2000 (Wang and Xu 2009), the pH value of the precipitation showed a remarkable

284   increase in recent years. For instance, the pH value in the precipitation of SWC increased from 3.5-

285   4.0 (the mean value of 1980-2000) to 5.87 during 2011-2016. Although some cities in Hunan and

286   Hubei province (e.g., Chengzhou, Erzhou) still suffered from the severe acid deposition, the mean

287   pH values (4.46) of the two provinces during 2011-2016 were slightly higher than those in 1980-

288   2000 (3.5-4.0). It was well known that precipitation pH was associated with the SO_2 and NO_x

289   emissions (Pu et al., 2017). Due to the implementation of SO_2 control measurements since the 11th

290   Five-year Plan, the SO_2 column concentration over China displayed a marked decrease after 2007

291   based on Global Ozone Monitoring Experiment (GOME), reported by Gottwald and Bovensmann

292   (2011). Based on the bottom-up method, Lu et al. (2010) also supposed that SO_2 emission began to

293   decrease since 2007, in good agreement with the results obtained from the remote sensing. Besides,

294   nearly all of the power plants built newly and the in-use plants have been required to be equipped

295   with advanced selective catalytic reduction (SCR) or selective non-catalytic reduction (SNCR) since

296   2010 (Tian et al., 2013; Lu et al., 2011), resulting in a gradual decrease of the NO_x emission after

297   2010 (China Statistical Yearbook, http://data.stats.gov.cn/easyquery.htm?cn=C01). Based on the

298   result of correlation analysis (Tab. S2), the pH value showed the significantly negative correlation

299   with SO_2 and NO_2 in the ambient air especially with the increased RH. Thus, it could be proposed

300   that the pH value of the precipitation in most of the regions of China during 2011 and 2016 were

301   significantly higher than those before 2000 because the SO_2 and NO_x emissions during 2011-2016

302   were lower than those before 2000.

303   The pH value in the precipitation at a national scale exhibited significantly seasonal variation

304 with the highest value in summer (6.57), followed by autumn (5.64), spring (5.49), and the lowest

305 one in winter (5.32) (Fig. 2b). The seasonal variation of pH values in wet deposition was supposed

306 to be linked with the wash-out effect of precipitation on atmospheric particular matters (Xing et al.,

307 2017), which was supported by the positive relevance between pH and precipitation ($p < 0.01$).

308 Besides, the scavenging atmospheric SO_2 by precipitation may also play an important role in the

309 seasonal variation of the pH values (Wu and Han, 2015). The atmospheric SO_2 concentration was

310 the lowest in summer and the highest in winter. The highest atmospheric SO_2 and sulfate

311 concentrations in winter of the north part of China were partially ascribed to the intensive domestic

312 coal combustion for heating (Liu et al., 2016b; Liu et al., 2017).

313 At a spatial scale across the whole China (Fig. 3a), the pH value of the precipitation presented a

314 gradual increase from SEC to NC and NWC. The relatively low pH values in the precipitation were

315 usually observed in YRD (i.e., Huzhou, Ningbo, and Shanghai), Hunan province (i.e., Changde,

316 Changsha, and Loudi), Hubei province (i.e., Wuhan), and Jiangxi province (i.e., Nanchang, Yichun,

317 and Jingdezhen), but the relatively high pH values occurred in NC and NWC, especially in Xinjiang

318 autonomous region (i.e., Changji, Altai, Urumqi and Aksu). Among of the 320 cities, the lowest one

319 and the highest one were located in Huzhou, (3.20, Zhejiang province), and Altai, (6.82, Xinjiang

320 autonomous region), respectively (Fig. 3). Compared with high acidity in some cities of SEC, the

321 acidity of the precipitation in many cities of NC could be largely neutralized by some alkaline ions

322 because the saline-alkali soils were widely distributed in NC (Wang et al., 2014). Some city

323 atmosphere (i.e., Urumqi and Altay) in Xinjiang autonomous region were frequently attacked by

324 local continental dust particles, diluting the precipitation acidity (Rao et al., 2015).

325 The annually mean EC varied from 10.18 ± 3.21 μS cm^{-1} to 13.33 ± 3.75 μS cm^{-1} during the

period (Fig. 2a). The EC value was mainly affected by total water-soluble ions in the precipitation

and rainfall amount, of which indirectly reflected the cleanliness of the precipitation and the air

pollution status. The decrease of EC in recent years suggested that air pollution in China has been

mitigated due to the implementation of special air pollution control measures (Wang et al., 2017;

Yang et al., 2016). The EC value also presented distinctly seasonal variation and showed the highest

value in spring (Fig. 2c), followed by ones in summer and autumn, and the lowest one in winter,

which was apparently different from the seasonal pH variation. Among all of the inorganic ions,

only Ca^{2+} displayed notable relationship with EC ($p < 0.01$). It was supposed that many crustal ions

such as Ca^{2+} could be lifted up and transported to East China by frequent dust storms in spring and

summer, thereby leading to the high EC value in the precipitation (Fu et al., 2014). The mean EC

value exhibited a significantly spatial variation with the higher ones in Shizuishan (36.60 $\mu S\ cm^{-1}$)

and Yinchuan (24.79 $\mu S\ cm^{-1}$) (Ningxia autonomous region), Wuwei (60.01 $\mu S\ cm^{-1}$) (Gansu

province), Edors (28.72 $\mu S\ cm^{-1}$) (Inner Mongolia autonomous region), and Aksu (22.06 $\mu S\ cm^{-1}$)

(Xinjiang autonomous region) and the lower one in some remote regions such as Lhasa (3.42$\mu S\ cm^{-1}$) (Tibet autonomous region), Aba (2.20 $\mu S\ cm^{-1}$) (Sichuan province) and Diqing (2.46) (Yunan

province) (Fig. 3b). The lowest and highest EC were observed in Aba (2.20 $\mu S\ cm^{-1}$) and Wuwei

(60.01 $\mu S\ cm^{-1}$), respectively (Fig. 3). The cities in the western and northern of Sichuan province,

and the southern of Tibet autonomous region presented the lower EC values due to the sparse

population and minimal industrial activity. Although TB has received the effects of the industrial

emissions and biomass burning from South Asia via a long-range atmospheric transport, most of the

pollutants tended to be deposited on the South of Himalayas except persistent organic pollutants

(POPs) (Yang et al., 2016b; Dong et al., 2017). The cities with higher EC was generally close to the

348   Taklamakan and Gobi deserts. Strong winds in these deserts stirred a large amount of dusts, and

349   then caused many dust events, resulting in high loading of Ca^{2+} and Mg^{2+} (Wang et al., 2016d). The

350   positive relationship between wind speed and EC also revealed that strong wind promoted the

351   accumulation of crustal ions over China (Tab. S2).

3.2 Chemical composition in the precipitation

3.2.1   The inter-annual variation of the water-soluble ions

354   The inter-annual variation of the ionic constitutes of the precipitation in China during 2011-2016

355   are summarized in Fig. 4. The concentrations of Na^+, NO_3^-, and SO_4^{2-} increased from 7.26 ± 2.51,

356   11.56 ± 3.71, and 33.73 ± 7.59 μeq/L to 11.04 ± 4.64, 13.59 ± 2.63, and 41.95 ± 8.64 μeq/L during

357   2011 and 2014, respectively (Fig. 4a). However, Na^+, NO_3^-, and SO_4^{2-} concentrations decreased

358   from the highest ones in 2014 to 9.75 ± 2.89, 12.29 ± 4.02, and 30.57 ± 7.43 μeq/L in 2016. The

359   concentrations of Ca^{2+}, NH_4^+, and Mg^{2+} increased from 31.59 ± 8.29, 14.84 ± 4.63, and 8.77 ± 2.42,

360   to 58.84 ± 10.31, 41.33 ± 10.26, and 10.49 ± 3.07 during 2011-2013 (Fig. 4a), whereas they

361   decreased from the peak values in 2013 to 31.20 ± 8.48, 18.13 ± 4.84, and 8.93 ± 2.92 μeq/L in

362   2016, respectively. The F^- concentration exhibited gradual decrease from 3.63 to 2.96 μeq/L during

363   2012-2016. However, the K^+ and Cl^- concentration fluctuated during 2011 and 2016 and did not

364   display regularly annual variation.

365   It was well documented that the SO_4^{2-} concentration was closely associated with the SO_2

366   emissions because SO_2 in the ambient air could be transformed into SO_4^{2-} during aging in the

367   atmosphere (Qiao et al., 2015). In the present study, SO_4^{2-} in the precipitation exhibited a marked

368   correlation with SO_2 in the ambient air ($p < 0.01$), especially with the increased RH (Tab. S2). The

369   total SO_2 emissions in China decreased dramatically due to the installation of the flue gas

370   desulfurization (FGD) systems and the closure of less efficient power plants in China since 2012

371   (Li et al., 2017b). At a national scale, the remarkable decrease of the SO_4^{2-} concentration was

372   observed since 2014, which lagged behind the decrease of the SO_2 emission. Such scenario was

373   widely observed in some developed countries such as Japan (Okuda et al., 2005). However, some

374   cities (i.e., Beijing and Baoding) in NC showed the notable decreases since 2012, which

375   corresponded to the decrease of the total SO_2 emission. It was supposed that the electrostatic

376   precipitators (ESP) and fabric filters (FFs) for the sulfates removal were more widely applied to

377   steel and iron plants, and cement production process, both of which were widely distributed in NC

378   (Hua et al., 2016; Wang et al., 2016b). Moreover, coal has been gradually replaced by natural gas

379   for domestic heating in Beijing, resulting in the less SO_2 emission and thus decreasing the SO_2

380   concentration in the ambient air (Pu et al., 2017). Based on the open data downloaded from National

381   Environmental Monitoring Platform, the annually mean SO_2 concentration in Beijing decreased

382   from 22.0 $\mu g/m^3$ to 9.29 $\mu g/m^3$ during 2014-2016, in good agreement with the temporal variation of

383   SO_4^{2-} in the precipitation.

384   The NO_x emission decreased rapidly after the upgrading of oil product quality standards, the

385   import denitrification facilities, and the implementation of low-NO_2 burner technologies (Li et al.,

386   2016; Liu et al., 2017). However, the NO_3^- concentration in the precipitation over China only

387   displayed slight decrease during this period, which was in good agreement with the slight decrease

388   of national NO_2 concentration in the atmosphere (Zhan et al., 2018). It suggested that stricter

389   controls on NO_x emissions from power plants might be counteracted by the increase of power plants

390   and energy consumption (Liu et al. 2015a; Wang et al. 2018). Besides, it was assumed that the high

391   NO_3^- in the precipitation resulted from the increase of motor vehicles (Link et al., 2017). Based on

392   the bottom-up method, the estimated NO_x emissions from vehicle exhausts in China linearly

393   increased by 75% since 1998 (Wu et al., 2016). Shandong suffered from the highest vehicle

394   emissions among all of the provinces, of which the NO_x released from vehicle exhausts in Shandong

395   province increased from 477.6 Gg to 513.8 Gg during 2011-2014 (Sun et al., 2016), corresponding

396   to the annual variation of NO_3^- in the precipitation of Jinan and Linyi. The NO_3^-/SO_4^{2-} value was

397   recognized as an important index to determine the relative importance of nitrate (mobile) vs. sulfate

398   (stationary) emission in the atmosphere (Arimoto et al., 1996). The value of NO_3^-/SO_4^{2-} at the

399   national scale was still lower than 1, suggesting that the contribution of sulfate to the acidity of the

400   precipitation was still higher than that of NO_3^-. Nevertheless, the ratio in the precipitation showed a

401   gradual increase from 0.33 to 0.40 during this period, indicating that the precipitation type in China

402   has evolved from sulfuric acid type to a mixed type controlled by sulfuric and nitric acid.

403   The NH_4^+ level in the precipitation was closely linked to the NH_3 emission because NH_3 tended

404   to be neutralized to form $(NH_4)_2SO_4$ and NH_4NO_3 in the atmosphere (Zhang et al., 2016). The

405   anthropogenic emission of NH_3 was mainly derived from fertilizer use, livestock manures, vehicle

406   exhausts, and industrial processes (Kang et al., 2016). Wherein, livestock manures and synthetic

407   fertilizer application were considered as two major source of the NH_3 emission, accounting for 80-

408   90% of total emission (Kang et al., 2016; Xu et al., 2016). The nitrogen fertilizer consumption has

409   decreased since 2013 (http://www.stats.gov.cn/), which was in good agreement with the variation of

410   the NH_4^+ concentration in the precipitation. Therefore, the fertilizer consumption could be treated

411   as an important factor for the NH_4^+ level in the precipitation. However, the NH_3 emission from

412   livestock manures estimated by Kang et al. (2016) showed an opposite variation to the NH_4^+ level

413   in the precipitation collected herein. It was probably attributed to the slight decrease of air

414   temperature in the major cities of China during 2011-2013 because the actual NH_3 emission to the

415   atmosphere was sensitive to air temperature (Kang et al., 2016), which has been proved by the

416   correlation analysis (Tab. S2). Apart from the contribution source mentioned above, soil served as

417   major natural sources of the NH_3 emissions (Sun et al., 2014). Teng et al. (2017) demonstrated that

418   urban green space made a great contribution to the NH_3 amount in the atmosphere. In the present

419   study, the urban green space in some cities such as Lianyungang (Jiangsu province) and Qingdao

420   (Shandong province) showed the marked correlation with the NH_4^+ level in the wet deposition.

421   The long-range transport of dust aerosol was considered as the major source of Ca^{2+} and Mg^{2+}

422   in the atmosphere (Fu et al., 2014). Song et al. (2016) reported that the magnitude of dust emissions

423   in spring generally decreased in the past decades. The dust deposition and ambient PM_{10}

424   concentration in the Xinjiang autonomous region also decreased dramatically during 2000-2013

425   (Zhang et al., 2017a). Here, Ca^{2+} and Mg^{2+} in the wet deposition of some cities such as Aksu in

426   Xinjiang autonomous region decreased from 32.37 to 4.80 µeq/L and from 15.80 to 4.81 µeq/L

427   during 2011-2016, respectively, corresponding to the decrease of dust deposition. However, the

428   decrease of Ca^{2+} and Mg^{2+} over China significantly lagged behind the reduction of dust deposition.

429   It was well known that the increase of soil particles and dusts due to urbanization might induce the

430   high level of Ca^{2+} and Mg^{2+} in the wet deposition (Lyu et al., 2016). The road mileage in China

431   increased by 25% from 2011 to 2013, while it only showed slight increase (2.52%) during 2013-

432   2016 (http://www.stats.gov.cn/). Padoan et al. (2017) also demonstrated that the resuspension of

433   road dust generally showed the highest impact on the emission of the Ca and Mg elements among

434   non-exhaust sources (i.e. tire wear, brake wear, road dust).

435   Both of K^+ and Cl^- were identified as the important tracers for biomass burning and fireworks

436   (Cheng et al., 2014). Nevertheless, the K^+ and Cl^- concentration in the precipitation did not reflect

437   the contribution of biomass burning because biomass burning usually occurred in dry seasons (Zhou

438   et al., 2017b). Furthermore, the K^+ concentration in the precipitation showed significantly

439   relationship with crustal ions (Ca^{2+} (r = 0.40, p < 0.01) and Mg^{2+} (r = 0.49, p < 0.01)) (Tab. S2),

440   suggesting that other sources could play important role on the accumulation of K^+ and Cl^-. Chen et

441   al. (2017b) recommended that fugitive dust to be the main source of K^+ when the mitigation

442   measures were seriously implemented. The minor F^- in the wet deposition served as an indicator of

443   coal combustion because fluorine was generally released from coal combustion (Chen et al., 2013).

444   Recently, the F^- emission displayed remarkable decrease because more coal-fired power plants were

445   equipped with FGD and dust removal equipment (Zhao and Luo, 2017), which explained the

446   decrease of F^- in the precipitation of some industrial cities such as Baoding (3.22 to 1.65 during

447   2012-2016), Shijiazhuang (3.18 to 2.73), and Handan (3.88 to 3.53) in Hebei province. Na^+ was

448   generally originated from the transport of sea salt aerosols, fugitive dusts, and the incineration of

449   wastes and fossil fuels (Zhao et al., 2011). The Cl^-/Na^+ value in the precipitation of some coastal

450   cities (i.e. Lishui (1.15), Jiaxing (1.20), Dandong (1.18), Wenzhou (1.18)) were similar to the marine

451   equivalent Cl^-/Na^+ ratio (1.17) (Wang et al., 2015a), suggesting that Na^+ in the precipitation of these

452   coastal cities might be derived from ocean. However, the Cl^-/Na^+ ratios in the precipitation of some

453   regions far from the ocean were significantly higher than marine equivalent Cl^-/Na^+ ratio due to the

454   contribution of coal combustion (Liu et al., 2016b; Liu et al., 2017).

455   3.2.2 The seasonal variation of the inorganic ions in the wet deposition

456   Overall, the mean concentrations of SO_4^{2-}, NO_3^- and F^- in the wet deposition were in the order

457   of winter (SO_4^{2-}, NO_3^- and F^-: 45.74, 19.44 and 6.10 μeq/L) > spring (42.61, 13.83, and 3.45 μeq/L) >

458   autumn (28.85, 9.73, and 2.67 μeq/L) > summer (19.26, 7.66, and 2.04 μeq/L) (Fig. 4b). However,

459   the seasonal variation of inorganic ions still showed the slight difference between North China and

460   South China. The mean concentrations of SO_4^{2-}, NO_3^- and F^- in the precipitation of North China

461   displayed the highest in winter (47.88, 13.79, and 5.24 μeq/L), followed by those in spring (47.02,

462   10.18, and 3.64 μeq/L), autumn (32.20, 10.08, and 2.73 μeq/L), and summer (22.75, 6.29, and 1.69

463   μeq/L). However, NO_3^- in South China showed the highest level in spring (27.66 μeq/L). It was well

464   known that SO_4^{2-} and NO_3^- were usually generated via the oxidation of SO_2 and NO_2 in the

465   atmosphere, respectively (Yang et al., 2016). The combustion of fossil fuels for domestic heating in

466   winter probably promoted the accumulations of SO_2 and NO_2 in the atmosphere (Liu et al., 2017;

467   Lu et al., 2010). The cities in North China showed the higher SO_4^{2-} and NO_3^- levels in the

468   precipitation of winter compared with those in summer, which were in agreement with the seasonal

469   variations of SO_2 and NO_2 concentrations in the ambient air. It reflected that the combustion of

470   fossil fuels for domestic heating contributed to the accumulation of SO_4^{2-} and NO_3^- and these ions

471   deposited via the rainfall. Nevertheless, the acidic ions in the cities of South China were not always

472   in agreement with those in North because coal combustion for heating in winter was not widespread.

473   The NO_3^- level in South China showed the highest one in spring due to the effects of meteorological

474   factors. The stagnant meteorological conditions including shallow mixing layers, high atmospheric

475   pressure, low precipitation, and low wind speed occurred frequently in winter, thereby trapping

476   more pollutants and elevating the concentrations of SO_2 and NO_2 in the atmosphere (Tai et al., 2010).

477   In contrast, strong solar radiation and turbulent eddies from ocean in summer could promote the

478   dispersion of these pollutants (Antony Chen et al., 2001). For instance, some coastal cities such as

479   Beihai (Guangxi autonomous region) and Haikou (Hainan province) were generally exposed of

480 strong solar radiation and high wind speed, which significantly decreased the SO_4^{2-} and NO_3^-

481 concentrations in the precipitation of summer (Beihai: SO_4^{2-} (6.06) and NO_3^- (7.37); Haikou: SO_4^{2-}

482 (5.33) and NO_3^- (4.96)), whereas they usually displayed the higher value in spring due to the scarce

483 rainfall amount. The F^- concentration in the precipitation displayed the similarly seasonal variation

484 to SO_4^{2-} and NO_3^-, which was likely associated with the higher coal consumption for domestic

485 heating in some industrial cities of NC, NWC, and NEC (Ding et al., 2017).

486   The concentrations of Cl^-, Ca^{2+}, K^+, NH_4^+, Mg^{2+}, and Na^+ exhibited the highest values in summer,

487 followed by those in spring and autumn, and the lowest one in winter. The higher concentration of

488 NH_4^+ in the precipitation collected in summer was probably linked to agricultural activities. The

489 widespread utilization of fertilizer in summer have been observed over China (Zhang et al., 2011;

490 Tao et al., 2016), which could increase the NH_3 emission. In addition, the NH_3 emission was

491 sensitive to the air temperature and generally increased with the temperature (Kang et al., 2016).

492 The NH_3 released from agricultural activities could transform to NH_4^+, especially under the

493 condition of high RH (Li et al., 2013). Thus, the high NH_3 emission and rapid photochemical

494 reaction contribute to the higher NH_4^+ in the precipitation in summer. However, K^+, Ca^{2+}, and Mg^{2+}

495 displayed higher concentrations in spring and summer, which was probably related to the high

496 loading of fugitive dusts (Zhang et al., 2017c). Lyu et al. (2016) demonstrated that the high

497 temperature coupled with strong wind caused the lower water content in the road, leading to higher

498 tendency of dust re-suspension in the Wuhan summer. In the present study, these crustal ions in the

499 precipitation also showed the higher values in the summer of Wuhan. The high concentration of Na^+

500 and Cl^- in spring and summer was probably attributed to the evaporation of sea salt under the

501 condition of high air temperature (Grythe et al., 2014). It was found that Na^+ in summer were 5.1-

502   10.3 times of those in winter in some coastal cities such as Qingdao (5.96) (Shandong province),

503   Qinhuangdao (9.65) (Hebei province), and Sanya (6.83) (Hainan province).

504   3.2.3 Spatial distribution of the water-soluble ions across the whole China

505   At a spatial scale, the annual mean concentrations of NO_3^-, Cl^-, Ca^{2+}, K^+, F^-, NH_4^+, Mg^{2+}, SO_4^{2-},

506   and Na^+ ranged from 0.20 to 47.98 μeq/L, from 0.27 to 80.86 μeq/L, from 0.59 to 157.15 μeq/L,

507   from 0.15 to 23.43 μeq/L, from 0.11 to 11.64 μeq/L, from 0.20 to 84.24 μeq/L, from 0.28 to 39.30

508   μeq/L, from 0.29 to 191.95 μeq/L, and from 0.15 to 39.50 μeq/L during 2011-2016, respectively.

509   All of these water-soluble ions displayed significantly spatial variation, as shown in Fig. 5 and Fig.

510   6.

511   The mean concentrations of the secondary ions (NO_3^-, NH_4^+, and SO_4^{2-}) showed the highest

512   values in YRD (Changzhou (34.53, 73.40, and 80.47 μeq/L) (Fig. 5a-c) and Nanjing (35.62, 17.12,

513   and 49.51 μeq/L) and SB (Chengdu (38.08, 65.19, and 57.16 μeq/L) and Leshan (25.32, 38.99, and

514   61.24 μeq/L)), followed by ones in NC (Jinan (11.67, 16.57, and 58.28 μeq/L) and Anyang (20.46,

515   41.32, and 22.01 μeq/L), and the lowest ones in TB (0.50, 0.91, and 1.44 μeq/L) (Lhasa). Many

516   secondary ions exhibited the high concentrations in YRD because of intensive energy consumption

517   and industrial activities (Zhou et al., 2017a). For instance, the total energy consumption of the

518   Jiangsu province was second to Hebei province among all of the provinces in China (Wang 2014).

519   The SO_2 and NO_x emissions from cement plants and iron and steel industries in Jiangsu and Zhejiang

520   province were significantly higher than those in other provinces (Hua et al., 2016; Wang et al.,

521   2016b), which was in coincident to the spatial agglomeration of the SO_2 and NO_2 concentrations in

522   the ambient air of these provinces It has been reported that the acid deposition pattern have moved

523   from SWC to SEC since 2000s (Yu et al., 2017a). However, SB still possessed high concentrations

524 of secondary ions in the precipitation because of high S content in the local consumed coals (Ren et

525 al., 2006). Besides, the unique topographic conditions and unfavorable diffusion conditions

526 facilitated the deposition of regionally transported pollutants stuck by Qinling mountains and Daba

527 mountain (Kuang et al., 2016), although the energy consumption of Sichuan province was much

528 less than those in other provinces (Tian et al., 2013). Moreover, the steady increase use of fertilizer

529 and livestock manures coupled with high air temperature made SB to be one of the NH_3 emission

530 hotspots (Li et al., 2017a). Nevertheless, some remote areas in NWC and SWC such as Lhasa and

531 Aba showed the lower secondary ions due to sparse population and anthropogenic activities (Li et

532 al., 2007). In these regions, these secondary ions were mainly derived from crustal source, and then

533 deposited concurrently in the rainfall events (Niu et al., 2014). Besides, relatively extensive

534 anthropogenic activities such as increased vehicle exhaust might promote the emissions of

535 secondary ions in the tourist season (Qiao et al., 2017). For instance, the number of tourists in Lhasa

536 have been increasing to 11 million until 2015 (http://www.xinhuanet.com/fortune/2016-

537 01/13/c_1117763885.htm), which could boost the slight increase of secondary ions in the wet

538 deposition.

539   F^- showed the higher concentrations in NC, YRD, and SB because many coal-fired power plants

540 and iron and steel industries were mainly concentrated in the Hebei and Jiangsu province (Liu et al.,

541 2015a) (Fig. 6a). Besides, Hebei and Jiangsu were two provinces with much higher coal

542 consumptions (Li et al., 2017), which could release large quantity of F^- to the atmosphere. Although

543 the power plants and iron and steel industries were relatively scarce in SB, many large phosphorite

544 mines might increase the F^- concentration in the precipitation (Wu et al., 2014). As one of the largest

545 phosphorite mine over China, Jinhe phosphorite mine was close to Chengdu, which significantly

546   increased the F^- concentration in the precipitation of Chengdu (9.21 μeq/L). Moreover, the high

547   abundance of F^- in the local coal (Mianyang: 269.25 μg/g, Guangan: 1061μg/g) also contributed to

548   the F^- emissions (Dai and Ren, 2006; Wang et al., 2016c; Ren et al., 2006). In addition, the F^- in the

549   precipitation showed remarkable relevance with T_{max} based on the correlation analysis (r = 0.12, p

550   < 0.05). The annually mean air temperature in SB (17.2 °C) were slightly higher than that in Hebei

551   (14.3 °C) and Jiangsu (16.4 °C) province, thereby boosting the F^- emission.

552   The high concentrations of Cl^- were mainly concentrated on coastal cities such as Shanghai,

553   Lianyungang (Jiangsu province) and Qingdao (Shandong province) (Fig. 6b), indicating the effect

554   of sea-salt sourced from the ocean (Gu et al., 2011; Allen et al., 2015; Grythe et al., 2014). The high

555   Na^+ concentration not only focused on these coastal cities (Fig. 6c), but also enrich in some arid and

556   semi-arid cities such as Jinchang (35.08 μeq/L) and Gannan (25.51 μeq/L) (Gansu province). It was

557   assumed that the windblown dust originated from Taklimakan Desert could play a vital role on the

558   enrichment of Na^+ in Inner Mongolia and Hexi corridor because these regions were located on the

559   downwind direction of dust (Engelbrecht et al., 2016). Meanwhile, the evaporation of salt lakes in

560   West China might promote the Na^+ enrichment in the precipitation (Bian et al., 2017). Besides, the

561   dust event also promoted the elevation of Ca^{2+}, especially in Jiayuguan and Guyuan (Gansu province)

562   (Fig. 6d), both of which were located in the Hexi corridor (Allen et al., 2015). The Mg^{2+} presented

563   higher value in some cities (Handan: 36.63 μeq/L, Liupanshui: 39.30 μeq/L) in the Hebei province

564   and Guizhou province (Fig. 6e). The soil in the Guizhou province possessed the highest Mg

565   concentration (843.33 mg/kg) in China (Li et al., 1992), where the Mg^{2+} stored into the soils could

566   be lifted into the atmosphere by strong wind coupled with severe stony desertification (Jiang et al.,

567   2014). Although the Mg concentration in the soil of Hebei province was slightly lower compared

568   with those of Guizhou province, the bioavailable Mg concentration peaked in Hebei province (Hao

569   et al., 2016), which could be inclined to re-suspend into the atmosphere and then deposit with the

570   rainfall in the warm season.

571   3.2.4 Neutralization capacity of the alkaline ions

572   In order to reveal the most important ion for neutralization (Ca^{2+}, NH_4^+, and Mg^{2+}) in the

573   precipitation, the relative proportion of three NFs in all of the cities are summarized in Fig. 7. The

574   triangular diagram showed that the contribution of three ions were in the order of Ca^{2+} (51.84%) >

575   NH_4^+ (34.14%) > Mg^{2+} (14.02%). The NF ratios of NH_4^+ and Ca^{2+} in China displayed the highest

576   values in summer, followed by ones in spring and autumn, and the lowest one in winter (Fig. 7a). It

577   was supposed that strong acid neutralization were mainly brought about by the alkaline ions via

578   high rainfall. Besides, the neutralization capacity of the alkaline ions reached higher in spring due

579   to the effects of dust events (Wang et al., 2015b). In the present study, the NFs of NH_4^+ and Ca^{2+} in

580   Beijing (NH_4^+: 0.57, Ca^{2+}: 0.17) and Baoding (NH_4^+: 0.56, Ca^{2+}: 0.19) showed the markedly higher

581   values in spring. Zhai and Li (2003) also observed that most frequent dust storms generally occurred

582   in NC in spring. However, the NFs of Mg^{2+} (0.70) showed the highest one in winter. Aside from the

583   temporal difference of neutralization, the NFs presented a significantly spatial variation in China

584   (Fig. 7b). The high NFs of Ca^{2+} were mainly concentrated on some cities in NWC such as

585   Bayingolin (0.57) because these arid and semi-arid regions were exposed of periodic Asian dust

586   intrusions (Yu et al., 2017b). In the case of the typical dust events, the content of crustal species

587   such as Ca increased substantially (Chen et al., 2015). Compared with the other regions, the NFs of

588   NH_4^+ showed the higher value in some cities of SWC such as Chengdu (0.55). Kang et al. (2016)

589   demonstrated that the NH_3 emissions in Sichuan province were significantly higher than those in

590 other provinces of China, accounting for more than 10 % of the total emission from livestock

591 manures. The NFs of Mg^{2+} peaked in NC, which was in good agreement with the higher

592 concentration of Mg^{2+} in the wet deposition of NC. The higher concentration of bioavailable Mg^{2+}

593 in the soil was beneficial to increase the neutralization capacity of Mg^{2+} in the wet deposition (Hao

594 et al., 2016), although the SO_2 and NO_2 emissions in NC were significantly higher than those in

595 other regions (Fu et al., 2016).

596 3.3 Comparisons of pH, EC, and the inorganic ion concentrations with the previous studies

597   The annual mean pH, EC and the inorganic ion levels in the precipitation of some metropolitans

598 across China are summarized in Tab. 1. The mean pH values of the most cities in SEC and SWC

599 (i.e., Shanghai: 4.39 and Wuhan: 4.68) were lower than those in some remote areas such as

600 Jiuzhaigou (5.95) and Yulong mountain (5.94) (Qiao et al., 2018; Niu et al., 2014), while the average

601 pH values of some cities in NC and NWC such as Zhengzhou (6.09) and Urumqi (6.13) were slightly

602 higher than those in remote areas. It was assumed that the remote areas were less affected

603 anthropogenic source except local tourist activities, while high aerosol emissions were mainly

604 centered on some metropolitans of SEC and SWC. The pH of the precipitation in Zhengzhou (pH =

605 6.09) (Henan province) and Urumqi (pH = 6.13) (Xinjiang autonomous region) showed high value

606 compared with some remote regions because of the strong neutralization capacity of alkaline ions

607 (Wang et al., 2014). Besides, the pH values in the wet deposition of most metropolitans in China

608 were also lower than those in some developing countries (e.g., Guaiba: 5.92, Petra: 6.80) (Tab. 1).

609 It was supposed that SO_2 and NO_x emitted from industrial and vehicle emissions in China could be

610 higher than those in some countries such as Brazil and Jordan (Wu and Han 2015). In addition,

611 higher abundance of the neutralizing components in Jordan tended to increase pH of the

612 precipitation. On the other hand, the pH values of the wet deposition in most cities of China were

613 significantly higher than those in some cities of developed countries such as Sardinia (pH = 5.18)

614 (Italy) and Adirondack (pH = 4.50) (United States). It was assumed that many Western countries

615 were faced up with severe acid issue due to the rapid industrialization before 2002 (Sickles II and

616 Shadwick 2015). In addition, the annually mean rainfall amount in some cities of East China were

617 higher than those in Sardinia and Adirondack, which could dilute the acidity of the precipitation

618 (Tsai et al., 2011). The mean EC in the wet deposition of most cities over China were approximate

619 to those in some remote regions (i.e., Yulong Mountain, Jiuzhaigou), and some foreign cities such

620 as Guaiba, Brazil. However, Lanzhou (EC = 58.06 $\mu S\ cm^{-1}$) (Gansu province) and Petra (EC = 160

621 $\mu S\ cm^{-1}$) (Jordan) showed remarkably higher value than other cities, suggesting that the dust

622 cyclones from Taklamakan and Khamaseen played vital roles on the EC and chemical composition

623 in the precipitation (Abed et al., 2009).

624   The concentrations of NO_3^-, SO_4^{2-}, and NH_4^+ in the most cities of China except Qingdao

625 (Shandong province) and Lhasa (Tibet autonomous region) were significantly higher than those in

626 some natural reserve areas such as Jiuzhaigou, Yulong Mountain, and Nam Co (Qiao et al., 2018;

627 Niu et al., 2014) (Tab. 1), suggesting the local point and non-point emissions in these cities played

628 important roles on the concentrations of inorganic ions in the precipitation. However, the

629 concentrations of these inorganic ions in the most cities were lower than those in foreign cities such

630 as Singapore, Petra (Jordan), Tokyo, and Newark (United States) (Balasubramanian et al., 2001; Al-

631 Khashman et al., 2005; Okuda et al., 2005; Song and Gao 2009), indicating the effects of restricting

632 emissions of air pollutants since Chinese 12th Five-Year Plan (Liu et al., 2016a). However, some

633 cities including Shenyang (Liaoning province) and Chengdu (Sichuan province) were still faced up

634   with severe acid deposition. On the whole, the concentrations of the crustal ions (Ca^{2+} and Mg^{2+})

635   were in the order of the arid and semi-arid cities/regions (Nam Co, Urumqi, Lanzhou, and Petra) >

636   the inland cities and natural reserve regions (Chengdu and Yulong mountain) > the coastal cities

637   (i.e., Guaiba, Singapore, and Tokyo). Kang et al. (2016) reported that Tibetan Plateau have been

638   frequently affected by dust events under the condition of climate change in the past decades, which

639   probably increased the Ca^{2+} and Mg^{2+} levels in Nam Co. However, it should be noted that some

640   coastal cities such as Patras (Greece) and Sardinia (Italy) possessed higher Ca^{2+} and Mg^{2+} levels,

641   which was probably attributed to the long transport of the dust from of the Sahara desert (Kabatas

642   et al. 2014). Cabello et al. (2016) demonstrated that African air masses mostly reached some coastal

643   cities of Mediterranean on the basis of back-trajectory analysis.

644   3.4 The source apportionment of the ions in the precipitation across China

645   3.4.1 EF and geochemical index method

646   The mean values of EFs (seawater and soil), SSF and CF in all of the cities are listed in Tab. 2.

647   The water-soluble ion was treated to be enriched relative to the reference source when the EF value

648   of the ion was significantly higher than 1.00, whereas it was considered to be diluted when the EF

649   value of the ion was not much higher than 1.00. In the present study, the mean EF_{sea} for Na^+, Cl^-,

650   SO_4^{2-}, NH_4^+, K^+, Mg^{2+}, Ca^{2+}, NO_3^-, and F^- over China were 1.00, 1.13, 7.22, 10.51, 16.16, 18.18,

651   231.56, 3507.49, and 5864.28, suggesting that Cl^- and Na^+ in the precipitation were enriched in the

652   marine origin at a national scale. The mean EF_{soil} of Mg^{2+}, K^+, Ca^{2+}, Na^+, SO_4^{2-}, F^-, NO_3^-, NH_4^+, and

653   Cl^- reached 0.55, 0.83, 1.00, 1.83, 5.13, 9.96, 59.36, 86.31, and 169.88, indicating that Ca^{2+}, K^+, and

654   Mg^{2+} were considered to be originated from the crustal source. Both of the EF_{sea} for SO_4^{2-} and NO_3^-

655   showed significantly spatial variability and they presented the higher ones in YRD and SB

656 (significantly higher than 1) (Fig. 8a-b), which suggested that both of the ions were not mainly

657 sourced from the sea source. However, EF_{sea} for SO_4^{2-} in some cities such as Nujiang (0.92) and

658 Nanchong (0.81) were lower than 1. It was assumed that the Indian monsoon played an important

659 role on the wet deposition of SO_4^{2-} (Gu et al., 2016). Except SO_4^{2-} and NO_3^-, EF_{sea} for other ions

660 showed relatively uniform distribution at a national scale. EF_{sea} for NH_4^+, F^-, Ca^{2+}, K^+, and Mg^{2+} in

661 most of the cities were higher than 1 (Fig. 8c and S1), indicating the effects of anthropogenic source

662 or crustal source. The EF_{sea} for Cl^- presented the lower value in many coastal cities such as Beihai

663 (0.53) and Haikou (0.52), while they were significantly higher than 1 in some inland cities such as

664 Daqing (13.11). The spatial variability of EF_{sea} for Cl^- confirmed the spatial difference of Cl^-/Na^+

665 between coastal cities and inland ones mentioned above. Compared with EF_{sea}, the EF_{soil} of ions

666 generally displayed remarkably spatial variation. The EF_{soil} of SO_4^{2-}, NO_3^-, F^-, and Cl^- showed

667 notably higher values in SEC, implicating the effects of industrial activity (Fig. 8a-b and S2a-b).

668 The EF_{soil} of NH_4^+ presented markedly higher value in the eastern region of Inner Mongolia and

669 Heilongjiang province such as Hegang (325.69) (Fig. 8c) because intensive grazing was beneficial

670 to the NH_3 emission (Kobbing et al., 2014). It was interesting to note that the EF_{soil} of Na^+ showed

671 higher value in some cities around Qinghai Lake and the evaporation of salt lake could contribute

672 to the higher EF_{soil} of Na^+ (Fig. S2c). The EF_{soil} of crustal ions such as Mg^{2+} and K^+ in NWC were

673 close to 1, reflecting the contributions of dust events and soils (Fig. S2e-f).

674   Based on the EF_{sea} and EF_{soil}, the estimated SSF, CF, and AF of ions are depicted in Fig. 9, S3,

675 and S4. The mean SSF values of NO_3^-, F^-, Ca^{2+}, NH_4^+, Mg^{2+}, K^+, SO_4^{2-}, Cl^-, and Na^+ were 0%,

676 0.02%, 0.06%, 0.10%, 2.94%, 4.88%, 13.85%, 88.31%, and 100%, respectively. The average CF

677 values of NH_4^+, NO_3^-, Cl^-, F^-, SO_4^{2-}, Na^+, K^+, Mg^{2+}, and Ca^{2+} reached 0.01%, 0.02%, 0.59%, 10.04%,

678   19.50%, 35.34%, 95.12%, 97.06%, and 99.94%, respectively. The AF value was considered to be

679   the contribution ratio of each ion except SSF and CF. The AF values of Ca^{2+}, K^+, Mg^{2+}, Na^+, Cl^-,

680   SO_4^{2-}, F^-, NH_4^+, and NO_3^- reached 0%, 0%, 0%, 0%, 11.10%, 66.65%, 89.94%, 99.89%, and 99.98%,

681   respectively. The results suggested that NO_3^-, SO_4^{2-}, NH_4^+, and F^- were mainly sourced from

682   anthropogenic activities based on minor SSF and CF. It was well documented that the combustion

683   of fossil fuels, iron and steel industrial emission, and vehicle exhaust were main sources of SO_4^{2-}

684   and NO_3^- across China (Song et al., 2006; Yang et al., 2016). In the present study, the AF values of

685   NO_3^- in all of cities were higher than 90%, and those of SO_4^{2-} in half of the cities were higher than

686   60%. Besides, the utility of nitrogen fertilization, and human and livestock excretions were treated

687   as the main source of NH_4^+ emission over China (Cao et al., 2009). Herein, 82.5% of cities across

688   China showed the higher AF value of NH_4^+ (> 90%). Ca^{2+}, K^+, and Mg^{2+} were mainly derived from

689   crustal origin based on the high CF values. Although the K^+ concentration in the fine particles was

690   usually sourced from biomass burning, the component in the coarse particles generally resulted from

691   the soil erosion and dust re-suspension (Cao et al., 2009). The higher CF values of K^+ in most of

692   cities in China such as Aksu (Xinjiang autonomous region) and Bayin (Gansu province) suggested

693   that the wet deposition has become the main removal mechanism for the K^+ in the coarse particles

694   (Lim et al., 1991). The Na^+ and Cl^- ions were mainly originated from sea source because they were

695   main components of sea-salt and sea-spray aerosol (Prather et al., 2013), which was also supported

696   by the higher SSF value.

697   At a spatial scale, the highest AF values of NO_3^-, SO_4^{2-}, NH_4^+, and F^- were mainly concentrated

698   on East China and SWC (Fig. 9a-c, S3a-c), which was similar to the spatial variation of population.

699   The emissions of aerosols and their precursors released by human activities were mainly

700   concentrated on East China (Fu and Chen 2016), thereby leading to high AF values of these

701   secondary ions. Indeed, many cities in NC such as Handan and Shijiazhuang showed the higher AF

702   value, which revealed the effects of power plant, non-ferrous smelting, and oral mining. The SSF

703   value of Cl^- exhibited high value in Xinjiang and Qinghai province (i.e., Altay and Haibei), SWC

704   (i.e., Chengdu and Guangan) (Fig. S3d-e), and some coastal cities (i.e., Ningbo and Shanghai). The

705   higher SSF values of Cl^- in SWC and coastal cities of East China were mainly controlled by Indian

706   monsoon and East Asia monsoon driven atmospheric transport, respectively (Gu et al., 2016).

707   However, it was assumed that the higher SSF value of Cl^- in the region close to Qinghai Lake could

708   be linked to the evaporation of saline (Bian et al., 2017). However, the relatively higher CF value

709   of Cl^- was centered on Ningxia autonomous region and Shaanxi province, which was frequently

710   exposed of Aeolian dust especially under the process of wind erosion (Lyu et al., 2017). As the

711   typical crustal ions, K^+ and Mg^{2+} in the most regions of China generally showed high CF values,

712   especially in some cities of SWC (i.e., Guiyang, Zunyi, Zhaotong) (Fig. S4a-d). It was supposed

713   that the severe soil erosion and loss, and rocky desertification frequently observed in Yungui Plateau

714   contributed to the higher CF value in this region (Jiang et al., 2014). The SSF of K^+ and Mg^{2+}

715   showed high values in some coastal cities (i.e., Sanya and Ningbo), and some cities of NWC such

716   as Haibei (Qinghai). The evaporation of salt in East China Sea and Qinghai Lake could play a vital

717   role on the K^+ and Mg^{2+} in these areas (Bian et al., 2017).

718   It should be noted that the geochemical index method showed some uncertainties for the

719   estimation of SSF, CF, and AF. First of all, the background values of Na^+ in the sea and Ca^{2+} in the

720   soil displayed the higher uncertainty, which varied significantly with the study areas. Unfortunately,

721   the background values of Na^+ and Ca^{2+} over China were absent. Besides, the source classification

722   might be not very accurate because many other sources such as forest fire, volcanic eruption were

723   ignored.

724   3.4.2 The FA-MLR analysis

725   In order to enhance the reliability of source identification, the FA method was also utilized to

726   identify the source of chemical compositions in the precipitation. The FA results of four seasons are

727   summarized in Tab. 3. Three principal components were extracted from the rainwater samples, all

728   of which explained 85.6% of the total variance. The Kaiser-Meyer-Olkin indicator (0.85) was higher

729   than 0.7, suggesting that three factors extracted in the present study was reasonable. Factor 1

730   grouped NO_3^- , F^-, NH_4^+, and SO_4^{2-}, accounting for 52.3% of the variance, which was generally

731   associated with dense anthropogenic activities (Nayebare et al., 2016; Zhang et al., 2017b). Factor

732   2 displayed high loadings of Na^+ and Cl^-, indicating the effects of sea-salt and sea-spray aerosol

733   (Gupta et al., 2015). The result was also in good agreement with the high SSF value of Na^+ and Cl^-

734   supported by geochemical index method. Factor 3 occupied 9.54% of the total variance and was

735   dominated by Ca^{2+}, Mg^{2+}, and K^+. The former two ions were considered to be the important

736   indicators of crustal origin or windblown dust source, which were commonly stored in soils and

737   dusts (Kchih et al., 2015). K^+ was also observed in urban fugitive dusts, although it was generally

738   considered as an important fingerprint of biomass burning (Shen et al., 2016). As a whole, the result

739   of FA was in coincident with that obtained from the EF and geochemical index method.

740   Although the key origins were isolated via the FA method, the contribution ratio of these

741   sources to the water-soluble ions were still unknown. Thus, the FA-MLR method was further applied

742   to quantify the contribution ratio of several sources to these ions in the 320 cities over China (Fig.

743   10a-d). In four seasons, the mean contributions of the anthropogenic source (NO_3^-, SO_4^{2-}, NH_4^+, and

744   F^-: 79.10%, 46.12%, 82.40%, and 71.02%) were significantly higher than those of sea source

745   (13.76%, 31.71%, 11.09%, and 11.52%) and crustal origin (7.14%, 22.17%, 6.52%, and 17.46%)

746   for NO_3^-, SO_4^{2-}, NH_4^+, and F^-. Nevertheless, the contribution ratio was in the order of crustal origin

747   (K^+, Ca^{2+}, and Mg^{2+}: 77.44%, 82.17%, and 70.51%) > anthropogenic source (13.91%, 10.20%, and

748   18.36%) > sea source (8.65%, 7.64%, and 11.14%) for K^+, Ca^{2+}, and Mg^{2+}. The sea source was the

749   dominant factor for the accumulation of Na^+ and Cl^- in the rainwater, followed by the crustal origin

750   and the anthropogenic source. In addition, the contribution ratios of three sources showed the slight

751   variation in different seasons (Fig. 10). For instance, the contribution ratio of sea source to most

752   inorganic ions especially Na^+ and Cl^- displayed the highest one in summer, followed by ones in

753   spring and autumn, and the lowest one in winter because the intense evaporation of sea salt in

754   summer was inclined to release more ions to the atmosphere (Teinilä et al., 2014). The contribution

755   ratio of anthropogenic activities presented the notable increase from summer to winter for SO_4^{2-}

756   because of dense coal combustion (20 kg coal/m^2) for domestic heating in winter (Zhao et al., 2016).

757   3.5 The deposition flux of the water-soluble ions and their key factors

758   At a national scale, the annually mean deposition fluxes of NO_3^-, Cl^-, Ca^{2+}, K^+, F^-, NH_4^+, Mg^{2+},

759   SO_4^{2-}, and Na^+ over China were 13.25, 8.44, 13.80, 2.49, 1.15, 5.90, 2.27, 33.41, and 4.39 kg ha^{-1}

760   yr^{-1} during 2011-2016. The deposition fluxes of NO_3^-, Ca^{2+}, K^+, NH_4^+, and Na^+ increased from 13.67

761   to 14.83 kg ha^{-1} yr^{-1}, 13.32 to 16.99 kg ha^{-1} yr^{-1}, 2.47 to 2.79 kg ha^{-1} yr^{-1}, 5.21 to 6.48 kg ha^{-1} yr^{-1},

762   and 4.17 to 5.74 kg ha^{-1} yr^{-1} from 2011 to 2013, respectively. However, they decreased to 13.65,

763   11.01, 2.52, 5.90, and 3.69 kg ha^{-1} yr^{-1} in 2016. The wet deposition fluxes of F^- and Mg^{2+} over China

764   decreased from 1.27 to 0.96 kg ha^{-1} yr^{-1} and 2.76 to 1.85 kg ha^{-1} yr^{-1} during 2012-2014, respectively.

765   However, they began to increase slightly to 1.17 and 2.15 in 2016, respectively. The wet deposition

766 fluxes of Cl^- and SO_4^{2-} showed gradual decrease from 9.80 and 38.87 kg ha^{-1} yr^{-1} to 8.09 and 26.54

767 kg ha^{-1} yr^{-1} during 2011-2016, respectively. On average, the wet deposition flux of NO_3^- were higher

768 by 2.25 times than that of NH_4^+, which was in contrast to the results of the dry deposition reported

769 by Xu et al. (2015). All of the water-soluble ions showed the highest wet deposition fluxes in

770 summer, followed by ones in spring and autumn, and the lowest ones in winter, which was probably

771 attributed by the high washout effect due to rain in summer (Jia et al., 2014). Based on the results

772 of the correlation analysis, the precipitation showed the significant relationship with the deposition

773 fluxes of the water-soluble ions ($p < 0.05$). In addition, the wet deposition fluxes of the water-soluble

774 ions showed the significantly spatial variation, which were in good agreement with the spatial

775 distribution of the water-soluble ion concentrations except Ca^{2+} (Fig. S5).

776   In order to determine the dominant factors affecting the wet deposition fluxes of the water-

777 soluble ions across China, GDP, GIP, TEC, N fertilizer use, vehicle ownership, UGS, dust days,

778 many meteorological factors (i.e., T_{max}, T_{min}, WS), and air pollutants (i.e., SO_2 and NO_2) were

779 introduced as the explanatory variables. The SR analysis results are depicted in Tab. 4. GIP, vehicle

780 ownership, NO_2, T_{min}, and wind speed served as the key factors affecting apparently the wet

781 deposition of NO_3^- at a national scale. The atmospheric emission of NO_x from coal-fired power

782 plants was estimated about 7489.6 kt in 2010, although many newly built power plants were

783 equipped with advanced low NO_x burner (LNB) systems (Tian et al., 2013). Zhang et al. (2014)

784 estimated that NO_x from vehicle emissions reached 4570 kt in 2008, which was considered as the

785 second NO_x source only to industrial activities. The NO_x released from anthropogenic activity could

786 enhance the NO_2 concentration in the ambient air, which could be also transformed to NO_3^- via

787 oxidation in the atmosphere, especially under the condition of high temperature and low WS (Zhang

et al., 2016). The wet deposition of NH_4^+ were affected by N fertilizer use, UGS, and NO_2 over

China. Russel et al. (1998) recommended early that NH_4^+ in the precipitation was most likely

derived from the N fertilizer use via an isotope techniques coupled with back trajectory analysis.

Besides, Teng et al. (2017) demonstrated that the emission from UGS was identified to contribute

to the atmospheric NH_3 significantly during 60% of the sampling times, which could increase the

NH_4^+ concentration in the precipitation due to the photochemical reaction. The wet deposition flux

of SO_4^{2-} was closely associated with TEC in the 320 cities of China, respectively. It was supposed

that the SO_2 emission were dependent on the use of coal and petroleum (Lu et al., 2010). While

terrestrial petroleum emissions have declined in recent years, the emissions from international

shipping have offset the decrease of terrestrial petroleum (Smith et al., 2011). In the present study,

the deposition of some crustal ions were linked to the dust days because they were mainly derived

from the dust storm or soil (Deshmukh et al., 2011; Zhang et al., 2011). The F^- deposition was

associated with GIP due to the contributions of the coal-fired power plant fly ash and industrial raw

material (Kong et al., 2011).

The GWR method was used to calculate the local regression coefficients in order to determine

the dominant factor affecting the deposition of the water-soluble ions at the regional scale (Fig. 11

and S6). The mean R^2 of GWR method was 0.50 over China, and the p value was lower than 0.05,

which suggested that the GWR method could be applicable to the study. The local regression

coefficient of dust days for crustal ions including Ca^{2+}, Cl^-, K^+, and Mg^{2+} increased from SEC to

NWC (Fig. S6a-e), suggesting that dust days played a significant role on the crustal ions in NWC

due to high intensity of dust deposition and extremely high WS (Zhang et al., 2017a). The influence

of GIP on the F^- and NO_3^- increased from West China to East China, and displayed the higher value

in some cities of YRD (i.e., Shanghai, Hangzhou) because many coal-fired power plants, cement plants, and municipal solid waste incineration plants were located in YRD (Hua et al., 2016; Tian et al., 2012; Tian et al., 2014) (Fig. S6f and 11a). The influence of N fertilizer use on NH_4^+ was concentrated on some cities of NEC such as Jiamusi (Heilongjiang province) (Fig. 11b-c), Harbin (Heilongjiang province), Changchun (Jilin province) because the largest commodity grain base were located in Heilongjiang and Jilin province, leading to the higher N fertilizer use (Cheng and Zhang, 2005). In contrast to the effects of GIP, the TEC influence increased gradually from SEC to NWC, and showed the highest value in Xinjiang autonomous region (i.e., Altay) (Fig. 11d). It has been demonstrated that an inverted U-shaped curve (Environment Kuznets Curve) between per capita GDP and energy consumption was generally observed during the development of economy (Song et al., 2013; Yang et al., 2017). The Environment Kuznets Curve denoted that the energy consumption displayed positive relationship with per capita GDP in the early stage of development. However, the positive relationship tended to transform into the negative relevance with the development of economy because the reliance on the energy-intensive industries would be reduced in the developed stage (Yang et al., 2017). It was assumed that Xinjiang autonomous region kept at the early stage of the inverted-U curve and largely rested on the energy-intensive industries as the less-developed province (Yang et al., 2017). However, some developed provinces in SEC such as Zhejiang and Jiangsu have sped up structural transformation of the economy and reduce the reliance on the heavy industries. The influence of UGS and vehicle ownership peaked in Shandong province (i.e., Qingdao, Jinan) and YRD (i.e., Shanghai, Hangzhou) (Fig. 11e-f). It was supposed that the UGS and vehicle ownership in these cities showed higher values among all of the 320 cities (National Bureau of Statistics of China). Apart from the effects of socioeconomic factors, the

832   meteorological factors also played significant roles on NO_3^-. The influences of air temperature and

833   WS both increased from East China to West China, and showed the highest values in Xinjiang

834   province (Fig. 11g-h). Zhang et al. (2017a) demonstrated that the strong dust events along with high

835   WS contributed to the neutralization of NO_3^-, although the NO_2 concentrations in some cities of

836   Xinjiang province were significantly higher than other regions of China.

837   **4. Conclusions**

838   This study newly reported spatiotemporal variation of nine water-soluble ions in the

839   precipitation across the whole China during 2011-2016. The mean pH and EC values varied

840   significantly compared with those during 1980-2000 because the implementation of special air

841   pollution control measures have mitigated the air pollution in China. The concentrations of Na^+,

842   NO_3^-, and SO_4^{2-} increased from 7.26 ± 2.51, 11.56 ± 3.71, and 33.73 ± 7.59 μeq/L to 11.04 ± 4.64,

843   13.59 ± 2.63, and 41.95 ± 8.64 μeq/L during 2011 and 2014, while they decreased from the highest

844   ones in 2014 to 9.75 ± 2.89, 12.29 ± 4.02, and 30.57 ± 7.43 μeq/L in 2016, respectively. The

845   concentrations of Ca^{2+}, NH_4^+, and Mg^{2+} increased by 86.26%, 178.50%, and 19.71% from 2011 to

846   2013, whereas they decreased from 58.84 ± 10.31, 41.33 ± 10.26, and 10.49 ± 3.07 in 2013 to 31.20

847   ± 8.48, 18.13 ± 4.84, and 8.93 ± 2.92 μeq/L in 2016, respectively. The concentration of F^- decreased

848   linearly by 5.58%/yr during 2012-2016. The mean concentrations of SO_4^{2-}, NO_3^- and F^- showed the

849   highest values in winter, followed by ones in spring and autumn, and the lowest ones in summer. It

850   was supposed that the dense anthropogenic activities such as domestic combustion for heating and

851   adverse meteorological conditions. The crustal ions (Ca^{2+}, Mg^{2+}, and K^+) peaked in spring and

852   summer, suggesting the contributions of fugitive dusts. The Na^+ and Cl^- were markedly affected by

853   evaporation of sea salt. All of the water-soluble ions in the precipitation exhibited notably spatial

854   variability. The secondary ions (SO_4^{2-}, NO_3^- and NH_4^+), and F^- peaked in YRD (i.e., Changzhou,

855   Hangzhou, and Nanjing) owing to the intensive energy consumption and industrial activities. The

856   higher S content in the coal and unfavorable diffusion conditions contributed to the higher

857   concentrations of secondary ions in SB (i.e., Chengdu, Leshan, and Dazhou). The crustal ions and

858   sea-salt ions showed the highest concentrations in semi-arid regions (i.e., Guyuan, Jiayuguan) and

859   coastal cities (i.e., Qingdao, Lianyungang), respectively.

860   The EF method, geochemical index method, and FA-MLR method consistently suggested that

861   NO_3^- , F^-, NH_4^+, and SO_4^{2-} were dominated by anthropogenic activities. However, the Na^+ and Cl^-

862   were closely associated with sea-salt aerosol. Ca^{2+}, Mg^{2+}, and K^+ were mostly derived from crustal

863   source. The results of SR analysis and GWR method implied that GIP, TEC, vehicle ownership, and

864   N fertilizer use were main factors for SO_4^{2-}, NO_3^-, NH_4^+, and F^- in the precipitation. However, the

865   crustal ions were significantly affected by dust events. The correlation between influential factors

866   and the ions in the wet deposition showed significantly spatial variability. The influence of dust days

867   on the crustal ions increased from SEC to NWC, whereas the influence of socioeconomic factors on

868   secondary ions showed the highest value in East China.

869   The present study validate the model estimations of the water-soluble ions deposition at a

870   national scale, and provide the fundamental data for the prevention and control of acid deposition

871   and air pollution. However, there were several plausible contributors to the uncertainty. First of all,

872   the monitoring sites were distributed unevenly and relatively scarce sites were located in Northwest

873   China. Moreover, the limited independent variables were included into the models. Thus, further

874   studies were required to establish more representative monitoring sites and incorporate more

875   variables to reduce the uncertainty associated with the ions deposition.

Author contributions

Rui Li analyzed the data and wrote the manuscript. Lulu Cui, Yilong Zhao, Ziyu Zhang, Tianming

Sun, Junlin Li, Wenhui Zhou, Ya Meng, and Kan Huang organized the campaign and analyzed data.

Hongbo Fu revised the manuscript.

Acknowledgements

This work was supported by National Key R&D Program of China (2016YFC0202700), National

Natural Science Foundation of China (Nos. 91744205, 21777025, 21577022, 21177026),

International cooperation project of Shanghai municipal government (15520711200), and Marie

Skłodowska-Curie Actions (690958-MARSU-RISE-2015). The meteorological data are avaiable at

http://data.cma.cn/. The socioeonomic data are collected from http://www.stats.gov.cn/.

References

Abed, A.M., Kuisi, M.A., Khair, H.A.: Characterization of the Khamaseen (spring) dust in Jordan, Atmos. Environ. 43, 2868-2876, https://doi.org/10.1016/j.atmosenv.2009.03.015, 2009.

AlKhatib, M. and Eisenhauer, A.: Calcium and strontium isotope fractionation during precipitation from aqueous solutions as a function of temperature and reaction rate; II. Aragonite. 209, 320-342, 2017.

Al-Khashman, O. A.: Study of chemical composition in wet atmospheric precipitation in Eshidiya area, Jordan, Atmos. Environ. 39(33), 6175-6183, https://doi.org/10.1016/j.atmosenv.2005.06.056, 2005.

Allen, H. M., Draper, D.C., Ayres, B.R., Ault, R., Bondy, A., Takahama, S., Modini, R.L., Baumann, K., Edgerton, E., and Knote, C.: Influence of crustal dust and sea spray supermicron particle concentrations and acidity on inorganic NO_3^- aerosol during the 2013 Southern Oxidant and Aerosol Study, Atmos. Chem. Phys., 15(18), 10669-10685, https://www.atmos-chem-phys.net/15/10669/2015/, 2015.

Aloisi, I., G. Cai, C. Faleri, L. Navazio, D. Serafini-Fracassini, and S. Del Duca.: Spermine regulates pollen tube growth by modulating Ca^{2+}-dependent actin organization and cell wall structure, Front Plant Sci, 8, 1701, 2017.

Antony Chen, L. W., B. G. Doddridge, R. R. Dickerson, J. C. Chow, P. K. Mueller, J. Quinn, and W. A. Butler.: Seasonal variations in elemental carbon aerosol, carbon monoxide and sulfur dioxide: Implications for sources, Geophys. Res. Lett., 28(9), 1711-1714, https://doi.org/10.1029/2000GL012354, 2001.

Arimoto, R., R. Duce, D. Savoie, J. Prospero, R. Talbot, J. Cullen, U. Tomza, N. Lewis, and B. Ray.: Relationships among aerosol constituents from Asia and the North Pacific during PEM‐West A, J. Geophys. Res., 101(D1), 2011-2023, https://doi.org/10.1029/95JD01071, 1996.

Bao, G., Q. Ao, Q. Li, Y. Bao, Y. Zheng, X. Feng, and X. Ding.: Physiological Characteristics of Medicago sativa L. in Response to Acid Deposition and Freeze-Thaw Stress, Water Air Soil Poll., 228(9),

376, 2017.

Balasubramanian, R., Victor, T., Chun, N.: Chemical and statistical analysis of precipitation in Singapore. Water Air Soil Poll. 130, 451-456, 2001.

Baumbach, G., Vogt, U.: Experimental determination of the effect of mountain-valley breeze circulation on air pollution in the vicinity of Freiburg. Atmos. Environ. 33, 4019-4027, https://doi.org/10.1016/S1352-2310(99)00143-0, 1999.

Beniston.: Environmental change in mountains and uplands, 2016.

Bian, S., D. Li, D. Gao, J. Peng, Y. Dong, and W. Li.: Hydrometallurgical processing of lithium, potassium, and boron for the comprehensive utilization of Da Qaidam lake brine via natural evaporation and freezing, Hydrometallurgy, 173, 80-83, 2017.

Bowden, R. D., E. Davidson, K. Savage, C. Arabia, and P. Steudler.: Chronic nitrogen additions reduce total soil respiration and microbial respiration in temperate forest soils at the Harvard Forest, Forest Ecol Manag., 196(1), 43-56, 2004.

Cao, Y.-Z., S. Wang, G. Zhang, J. Luo, and S. Lu.: Chemical characteristics of wet precipitation at an urban site of Guangzhou, South China, Atmos. Res., 94(3), 462-469, https://doi.org/10.1016/j.atmosres.2009.07.004, 2009.

Cabello, M., Orza, J.A.G., Duenas, C., Liger, E., Gordo, E., Canete, S.: Back-trajectory analysis of African dust outbreaks at a coastal city in southern Spain: Selection of starting heights and assessment of African and concurrent Mediterranean contributions, Atmos. Environ., 140, 10-21, https://doi.org/10.1016/j.atmosenv.2016.05.047, 2016.

Chen, J., C. Li, Z. Ristovski, A. Milic, Y. Gu, M. S. Islam, S. Wang, J. Hao, H. Zhang, and C. He.: A review of biomass burning: Emissions and impacts on air quality, health and climate in China, Sci. Total

Environ., 579, 1000-1034, https://doi.org/10.1016/j.scitotenv.2016.11.025, 2017a.

Chen, J., G. Liu, Y. Kang, B. Wu, R. Sun, C. Zhou, and D. Wu.: Atmospheric emissions of F, As, Se, Hg, and Sb from coal-fired power and heat generation in China, Chemosphere, 90(6), 1925-1932, https://doi.org/10.1016/j.chemosphere.2012.10.032, 2013.

Chen, P., T. Wang, X. Lu, Y. Yu, M. Kasoar, M. Xie, and B. Zhuang.: Source apportionment of size-fractionated particles during the 2013 Asian Youth Games and the 2014 Youth Olympic Games in Nanjing, China, Sci. Total Environ., 579, 860-870, https://doi.org/10.1016/j.scitotenv.2016.11.014, 2017b.

Chen, Y., B. Luo, and S.-d. Xie.: Characteristics of the long-range transport dust events in Chengdu, Southwest China, Atmos. Environ., 122, 713-722, https://doi.org/10.1016/j.atmosenv.2015.10.045, 2015.

Cheng, Y.-q., and P. Zhang.: Regional patterns changes of Chinese grain production and response of commodity grain base in northeast China, Scientia Geographica Sinica, 25(5), 514, 2005.

Cheng, Y., G. Engling, K.-b. He, F.-k. Duan, Z.-y. Du, Y.-l. Ma, L.-l. Liang, Z.-f. Lu, J.-m. Liu, and M. Zheng.: The characteristics of Beijing aerosol during two distinct episodes: Impacts of biomass burning and fireworks, Environ. Pollut., 185, 149-157, https://doi.org/10.1016/j.envpol.2013.10.037, 2014.

Chen, Z.J., Chen, C.X., Liu, Y.Q., Lin, Z.S.: The background values and characteristics of soil elements in Fujian province. Environ. Monit. China, 8, 107-110, 1992.

Cong, Z., S. Kang, and K. Kawamura (2016), The long-range transport of atmospheric aerosols from South Asia to Himalayas, paper presented at EGU General Assembly Conference Abstracts.

Clemens, S.: Toxic metal accumulation, responses to exposure and mechanisms of tolerance in plants, 88, 1707-1719, 2006.

Dai, S., and D. Ren.: Fluorine concentration of coals in China-an estimation considering coal reserves,

Fuel, 85(7), 929-935, 2006.

Deshmukh, D. K., M. K. Deb, Y. I. Tsai, and S. L. Mkoma.: Water soluble ions in $PM_{2.5}$ and PM_1 aerosols in Durg city, Chhattisgarh, India, Aerosol Air Qual. Res, 11, 696-708, 10.4209/aaqr.2011.03.0023, 2011.

Ding, X., L. Kong, C. Du, A. Zhanzakova, H. Fu, X. Tang, L. Wang, X. Yang, J. Chen, and T. Cheng.: Characteristics of size-resolved atmospheric inorganic and carbonaceous aerosols in urban Shanghai, Atmos. Environ., 167, 625-641, https://doi.org/10.1016/j.atmosenv.2017.08.043, 2017.

Dong, Z.W., Kang, S.C., Guo, J.M., Zhang, Q.G., Wang, X.J., Qi, D.H.: Composition and mixing states of brown haze particle over the Himalayas along two transboundary south-north transects, Atmos. Environ., 156, 24-35, https://doi.org/10.1016/j.atmosenv.2017.02.029, 2017.

Driscoll, C. T., K. M. Driscoll, M. J. Mitchell, and D. J. Raynal.: Effects of acidic deposition on forest and aquatic ecosystems in New York State, Environ. Pollut., 123(3), 327-336, https://doi.org/10.1016/S0269-7491(03)00019-8, 2003.

Du, E.Z., Vries, W.D., Galloway, J.N., Hu, X.Y., Fang, J.Y.: Changes in wet nitrogen deposition in the United States between 1985 and 2012, Environ. Res. Lett., 9, 095004, https://doi.org/10.1088/1748-9326/9/9/095004, 2014.

Emmett, B.: The impact of nitrogen on forest soils and feedbacks on tree growth, in Forest Growth Responses to the Pollution Climate of the 21st Century, edited, pp. 65-74, Springer, 1999.

Engelbrecht, P. J., Moosmüller, H., Pincock, S., Jayanty, R.K.M., Lersch, T., Casuccio, G.: Technical note: Mineralogical, chemical, morphological, and optical interrelationships of mineral dust re-suspensions. Atmos. Chem. Phys. 16, 10809–10830, https://www.atmos-chem-phys.net/16/10809/2016/, 2016.

Fornaro, A., Gutz, I.G.R.: Wet deposition and related atmospheric chemistry in the São Paulo metropolis,

Brazil: part 2-contribution of formic and acetic acids. Atmos. Environ. 37, 117-128, https://doi.org/10.1016/S1352-2310(02)00885-3, 2003.

Fu, H., G. Shang, J. Lin, Y. Hu, Q. Hu, L. Guo, Y. Zhang, and J. Chen.: Fractional iron solubility of aerosol particles enhanced by biomass burning and ship emission in Shanghai, East China, Sci. Total Environ., 481, 377-391, https://doi.org/10.1016/j.scitotenv.2014.01.118, 2014.

Fu, H.B., Chen, J.M.: Formation, features and controlling strategies of severe haze-fog pollutions in China, Sci. Total Environ., 578, 121-138, https://doi.org/10.1016/j.scitotenv.2016.10.201, 2016.

Garland, J.A.: Dry and wet removal of sulphur from the atmosphere, Sulfur in the Atmosphere, 349-362, 1978.

Gerson, J. R., C. T. Driscoll, and K. M. Roy.: Patterns of nutrient dynamics in Adirondack lakes recovering from acid deposition, Ecol. Appl., 26(6), 1758-1770, 2016.

Glavas, S., Moschonas, N.: Origin of observed acidic–alkaline rains in a wet-only precipitation study in a Mediterranean coastal site, Patras, Greece. Atmos. Environ. 36, 3089–3099, https://doi.org/10.1016/S1352-2310(02)00262-5, 2002.

Gottwald, M., Bovensmann, H.: SCIAMACHY: Exploring the Changing Earth's Atmosphere, first ed. Springer (ISBN 978-9-481-9895-5), 2011.

Grythe, H., J. Ström, R. Krejci, P. Quinn, and A. Stohl.: A review of sea-spray aerosol source functions using a large global set of sea salt aerosol concentration measurements, Atmos. Chem. Phys., 14(3), 1277, https://www.atmos-chem-phys.net/14/1277/2014/, 2014.

Gu, J., Pitz, M., Schnelle-Kreis, J., Diemer, J., Reller, A., Zimmermann, R., Soentgen, J., Stoelzel, M., Wichmann, H.E., Peters, A., Cyrys, J.: Source apportionment of ambient particles: comparison of positive matrix factorization analysis applied to particle size distribution and chemical composition data.

Atmos. Environ. 45, 1849-1857, https://doi.org/10.1016/j.atmosenv.2011.01.009, 2011.

Gu, Y., H. Liao, and J. Bian.: Summertime nitrate aerosol in the upper troposphere and lower stratosphere over the Tibetan Plateau and the South Asian summer monsoon region, Atmos. Chem. Phys., 16(11), 6641-6663, https://doi.org/10.5194/acp-16-6641-2016, 2016.

Gupta, D., H.-J. Eom, H.-R. Cho, and C.-U. Ro.: Hygroscopic behavior of $NaCl$-$MgCl_2$ mixture particles as nascent sea-spray aerosol surrogates and observation of efflorescence during humidification, Atmos. Chem. Phys., 15(19), 11273-11290, https://doi.org/10.5194/acp-15-11273-2015, 2015.

Hao, G.J., Zhou, J.Q., Fang, H.L.: Applicability of AB-DTPA method for determining the available content of multi-element in typical soils in China, Acta Agr. Shanghai (in Chinese), 32, 100-107, 2016.

Hua, S., H. Tian, K. Wang, C. Zhu, J. Gao, Y. Ma, Y. Xue, Y. Wang, S. Duan, and J. Zhou.: Atmospheric emission inventory of hazardous air pollutants from China's cement plants: Temporal trends, spatial variation characteristics and scenario projections, Atmos. Environ., 128, 1-9, https://doi.org/10.1016/j.atmosenv.2015.12.056, 2016.

Hunová, I., Maznová, J., Kurfürst, P.: Trends in atmospheric deposition fluxes of sulphur and nitrogen in Czech forests, Environ. Pollut., 184, 668-675, https://doi.org/10.1016/j.envpol.2013.05.013, 2014.

Ito, M., Mitchell, M., Driscoll, C.T.: Spatial patterns of precipitation quantity and chemistry and air temperature in the Adirondack region of New York. Atmos. Environ. 36, 1051–1062, https://doi.org/10.1016/S1352-2310(01)00484-8, 2002.

Jia, Y., G. Yu, N. He, X. Zhan, H. Fang, W. Sheng, Y. Zuo, D. Zhang, and Q. Wang.: Spatial and decadal variations in inorganic nitrogen wet deposition in China induced by human activity, Scientific Reports, 4, https://doi.org/10.1038/srep03763, 2014.

Jiang, Z., Y. Lian, and X. Qin.: Rocky desertification in Southwest China: impacts, causes, and

restoration, Earth-Science Reviews, 132, 1-12, https://doi.org/10.1016/j.earscirev.2014.01.005, 2014.

Kang, Y., M. Liu, Y. Song, X. Huang, H. Yao, X. Cai, H. Zhang, L. Kang, X. Liu, and X. Yan.: High-resolution ammonia emissions inventories in China from 1980 to 2012, Atmos. Chem. Phys., 16(4), 2043-2058, https://doi.org/10.5194/acp-16-2043-2016, 2016.

Kang, L.T., Huang, J.P., Chen, S.Y., Wang, X.: Long-term trends of dust events over Tibetan Plateau during 1961–2010, Atmos. Environ., 125, 188-198, https://doi.org/10.1016/j.atmosenv.2015.10.085, 2016.

Kabatas, B., Unal, A., Pierce, R.B., Kindap, T., Pozzoli, L.: The contribution of Saharan dust in PM_{10} concentration levels in Anatolian Peninsula of Turkey, Sci. Total Environ., 488-489, 413-421, https://doi.org/10.1016/j.scitotenv.2013.12.045, 2014.

Kchih, H., C. Perrino, and S. Cherif.: Investigation of desert dust contribution to source apportionment of PM_{10} and $PM_{2.5}$ from a southern Mediterranean coast, Aerosol Air Qual. Res. 15(2), 454-464, 10.4209/aaqr.2014.10.0255, 2015.

Keene, W. C., Pszenny, A. A. P., Galloway, J. N., and Hawley, M. E.: Sea-salt corrections and interpretation of constituent ratios in marine precipitation, J. Geophys. Res.-Atmos., 91, 6647–6658, https://doi.org/10.1029/JD091iD06p06647, 1986.

Kong, S., Y. Ji, B. Lu, L. Chen, B. Han, Z. Li, and Z. Bai.: Characterization of PM_{10} source profiles for fugitive dust in Fushun-a city famous for coal, Atmos. Environ., 45(30), 5351-5365, https://doi.org/10.1016/j.atmosenv.2011.06.050, 2011.

Kobbing, J.F., Patuzzi, F., Baratieri, M., Beckmann, V., Thevs, N., Zerbe, S.: Economic evaluation of common reed potential for energy production: a case study in Wuliangsuhai Lake (Inner Mongolia, China). Biomass Bioenerg. 70, 315-329, 2014.

Kulshrestha, U.C., Sarkar, A.K., Srivastava, S.S., Parashar, D.C.: Wet-only and bulk deposition studies at New Delhi (India). Water Air Soil Pollut., 85, 2137–2142, 1995.

Kuribayashi, M., T. Ohara, Y. Morino, I. Uno, J.-i. Kurokawa, and H. Hara.: Long-term trends of sulfur deposition in East Asia during 1981-2005, Atmos. Environ., 59, 461-475, https://doi.org/10.1016/j.atmosenv.2012.04.060, 2012.

Kuang, F.H., Liu, X.J., Zhu, B., Shen, J., Pan, Y., Su, M.: Wet and dry nitrogen deposition in the central Sichuan Basin of China, Atmos. Environ. 143, 39-50, https://doi.org/10.1016/j.atmosenv.2016.08.032, 2016.

Lawson, D.R., Winchester, J.W.: A standard crustal aerosol as a reference for elemental enrichment factors, Atmos. Environ. 13, 925-930, 1979.

Larssen, T., and G. Carmichael.: Acid rain and acidification in China: the importance of base cation deposition, Environ. Pollut., 110(1), 89-102, https://doi.org/10.1016/S0269-7491(99)00279-1, 2000.

Larssen, T., H. M. Seip, A. Semb, J. Mulder, I. P. Muniz, R. D. Vogt, E. Lydersen, V. Angell, T. Dagang, and O. Eilertsen.: Acid deposition and its effects in China: an overview, Environ. Sci. Poli., 2(1), 9-24, 1999.

Leng, Q.M., Cui, J., Zhou, F.W., Du, K., Zhang, L.Y., Fu, C., Liu, Y., Wang, H.B., Shi, G.M., Gao, M., Yang, F.M., He, D.Y.: Wet-only deposition of atmospheric inorganic nitrogen and associated isotopic characteristics in a typical mountain area, southwestern China, Sci. Environ. Total, 616, 55-63, https://doi.org/10.1016/j.scitotenv.2017.10.240, 2018.

Le Bolloch, O., Guerzoni, S.: Acid and alkaline deposition in precipitation on the western coast of Sardinia, Central Mediterranean (40 N, 81 E). Water Air Soil Poll. 85, 2155-2160, 1995.

Li, C.L., Kang, S.C., Zhang, Q.G., Kaspari, S.: Major ionic composition of precipitation in the Nam Co

region, Central Tibetan Plateau. Atmos. Res. 85, 351–360, https://doi.org/10.1016/j.atmosres.2007.02.006, 2007.

Li, L., Q. Tan, Y. Zhang, M. Feng, Y. Qu, J. An, and X. Liu.: Characteristics and source apportionment of $PM_{2.5}$ during persistent extreme haze events in Chengdu, southwest China, Environ. Pollut., 230, 718-729, https://doi.org/10.1016/j.envpol.2017.07.029, 2017a.

Li, R., L. Cui, J. Li, A. Zhao, H. Fu, Y. Wu, L. Zhang, L. Kong, and J. Chen.: Spatial and temporal variation of particulate matter and gaseous pollutants in China during 2014–2016, Atmos. Environ., 161, 235-246, https://doi.org/10.1016/j.atmosenv.2017.05.008, 2017b.

Li, X., L. Wang, D. Ji, T. Wen, Y. Pan, Y. Sun, and Y. Wang.: Characterization of the size-segregated water-soluble inorganic ions in the Jing-Jin-Ji urban agglomeration: Spatial/temporal variability, size distribution and sources, Atmos. Environ., 77, 250-259, https://doi.org/10.1016/j.atmosenv.2013.03.042, 2013.

Li, Y., J. Meng, J. Liu, Y. Xu, D. Guan, W. Tao, Y. Huang, and S. Tao.: Interprovincial reliance for improving air quality in China: a case study on black carbon aerosol, Environ. Sci. Technol., 50(7), 4118-4126, 10.1021/acs.est.5b05989, 10.1021/acs.est.5b05989, 2016.

Li, R., Li, J.L., Cui, L.L., Wu, Y., Fu, H.B., Chen, J.M., Chen, M.D.: Atmospheric emissions of Cu and Zn from coal combustion in China: Spatio-temporal distribution, human health effects, and short-term prediction, Environ. Pollut., 229, 724-734, https://doi.org/10.1016/j.envpol.2017.05.068, 2017.

Li, Z.Y., Wang, Z.L., Li, R.J., Xu, Q,H.: The analysis of element content in the soil of 29 provinces/municipality/autonomous region in China, Shanghai agriculture technology (in Chinese), 1992.

Li, Z., Ma, Z., vander Kuijp, T., Yuan, Z.W., Huang, L.: A review of soil heavy metal pollution from mines in China: Pollution and health risk assessment, Sci. Total Environ. 468-469, 843-853,

https://doi.org/10.1016/j.scitotenv.2018.06.068, 2014.

Lim, B., T. Jickells, and T. Davies.: Sequential sampling of particles, major ions and total trace metals in wet deposition, Atmospheric Environment. Part A. General Topics, 25(3-4), 745-762, 1991.

Link, M. F., J. Kim, G. Park, T. Lee, T. Park, Z. B. Babar, K. Sung, P. Kim, S. Kang, and J. S. Kim.: Elevated production of NH_4-NO_3 from the photochemical processing of vehicle exhaust: Implications for air quality in the Seoul Metropolitan Region, Atmos. Environ., 156, 95-101, https://doi.org/10.1016/j.atmosenv.2017.02.031, 2017.

Liu, F., S. Beirle, Q. Zhang, B. Zheng, D. Tong, and K. He.: NO_x emission trends over Chinese cities estimated from OMI observations during 2005 to 2015, Atmos. Chem. Phys., 17(15), 9261-9275, https://doi.org/10.5194/acp-17-9261-2017, 2017.

Liu, F., Q. Zhang, D. Tong, B. Zheng, M. Li, H. Huo, and K. He.: High-resolution inventory of technologies, activities, and emissions of coal-fired power plants in China from 1990 to 2010, Atmos. Chem. Phys., 15(23), 13299-13317, https://doi.org/10.5194/acp-15-13299-2015, 2015a.

Liu, Y. W., Ri, X., Wang, Y. S., Pan, Y. P., Piao, S. L.: Wet deposition of atmospheric inorganic nitrogen at five remote sites in the Tibetan Plateau, Atmos. Chem. Phys., 15, 11683-11700, https://doi.org/10.5194/acp-15-11683-2015, 2015b.

Liu, L., Zhang, X.Y., Wang, S.Q., Zhang, W.T., Lu, X.H.: Bulk sulfur deposition in China, Atmos. Environ., 135, 41-49, https://doi.org/10.1016/j.atmosenv.2016.04.003, 2016a.

Liu, P.F., Zhang, C., Mu, Y., Liu, C.T., Xue, C.Y., Ye, C., Liu, J.F., Zhang, Y.Y., Zhang, H.X.: The possible contribution of the periodic emissions from farmers' activities in the North China Plain to atmospheric water-soluble ions in Beijing, Atmos. Chem. Phys., 16, 10097-10109, https://doi.org/10.5194/acp-16-10097-2016, 2016b.

Liu, P.F., Zhang, C.L., Xue, C.Y., Mu, Y.J., Liu, J.F., Zhang, Y.Y., Tian, D., Ye, C., Zhang, H.X., Guan, J.: The contribution of residential coal combustion to atmospheric PM$_{2.5}$ in northern China during winter, Atmos. Chem. Phys., 17, 11503–11520, https://doi.org/10.5194/acp-17-11503-2017, 2017.

Liu, X., L. Duan, J. Mo, E. Du, J. Shen, X. Lu, Y. Zhang, X. Zhou, C. He, and F. Zhang.: Nitrogen deposition and its ecological impact in China: an overview, Environ. Pollut., 159(10), 2251-2264, https://doi.org/10.1016/j.envpol.2010.08.002, 2011.

Liu, X., X. Ju, Y. Zhang, C. He, J. Kopsch, and Z. Fusuo.: Nitrogen deposition in agroecosystems in the Beijing area, Agr. Ecosyst. Enviro., 113(1), 370-377, 2006.

Liu, X., Y. Zhang, W. Han, A. Tang, J. Shen, Z. Cui, P. Vitousek, J. W. Erisman, K. Goulding, and P. Christie.: Enhanced nitrogen deposition over China, Nature, 494(7438), 459, https://doi.org/10.1038/nature11917, 2013.

Lu, X., L. Y. Li, N. Li, G. Yang, D. Luo, and J. Chen.: Chemical characteristics of spring precipitation of Xi'an city, NW China, Atmos. Environ., 45(28), 5058-5063, https://doi.org/10.1016/j.atmosenv.2011.06.026, 2011.

Lu, X., Q. Mao, F. S. Gilliam, Y. Luo, and J. Mo.: Nitrogen deposition contributes to soil acidification in tropical ecosystems, Global Change Biol., 20(12), 3790-3801, https://doi.org/10.1111/gcb.12665, 2014.

Lu, Z., D. G. Streets, Q. Zhang, S. Wang, G. R. Carmichael, Y. F. Cheng, C. Wei, M. Chin, T. Diehl, and Q. Tan.: Sulfur dioxide emissions in China and sulfur trends in East Asia since 2000, Atmos. Chem. Phys., 10(13), 6311-6331, https://doi.org/10.5194/acp-10-6311-2010, 2010.

Luo, X.S., Xue, Y., Wang, Y.L., Cang, L., Xu, B., Ding, J.: Source identification and apportionment of heavy metals in urban soil profiles, Chemosphere., 127, 152-157, https://doi.org/10.1016/j.chemosphere.2015.01.048, 2015.

Lyu, X., N. Chen, H. Guo, L. Zeng, W. Zhang, F. Shen, J. Quan, and N. Wang.: Chemical characteristics and causes of airborne particulate pollution in warm seasons in Wuhan, central China, Atmos. Chem. Phys., 16(16), 10671-10687, https://doi.org/10.5194/acp-16-10671-2016, 2016.

Lyu, Y., Z. Qu, L. Liu, L. Guo, Y. Yang, X. Hu, Y. Xiong, G. Zhang, M. Zhao, and B. Liang.: Characterization of dustfall in rural and urban sites during three dust storms in northern China, 2010, Aeolian Res., 28, 29-37, 2017.

McGlade, C., Ekins, P.: The geographical distribution of fossil fuels unused when limiting global warming to 2 °C, Nature, 517, 187-190, https://doi.org/10.1038/nature14016, 2015.

Müller, W. E., E. Tolba, Q. Feng, H. C. Schröder, J. S. Markl, M. Kokkinopoulou, and X. Wang.: Amorphous Ca^{2+} polyphosphate nanoparticles regulate the ATP level in bone-like SaOS-2 cells, J. Cell Sci., 128(11), 2202-2207, 2015.

Migliavacca, D., E. Teixeira, F. Wiegand, A. Machado, and J. Sanchez.: Atmospheric precipitation and chemical composition of an urban site, Guaiba hydrographic basin, Brazil, Atmos. Environ., 39(10), 1829-1844, https://doi.org/10.1016/j.atmosenv.2004.12.005, 2005.

Mikhailova, E., M. Goddard, C. Post, M. Schlautman, and J. Galbraith.: Potential contribution of combined atmospheric Ca^{2+} and Mg^{2+} wet deposition within the continental US to soil inorganic carbon sequestration, Pedosphere, 23(6), 808-814, 2013.

National Bureau of Statistics of China, 2010-2016 (Chinese).

Négrel, P., C. Guerrot, and R. Millot.: Chemical and strontium isotope characterization of precipitation in France: influence of sources and hydrogeochemical implications, Isot. Environ. Healt., 43(3), 179-196, 2007.

Nayebare, S. R., O. S. Aburizaiza, H. A. Khwaja, A. Siddique, M. M. Hussain, J. Zeb, F. Khatib, D. O.

Carpenter, and D. R. Blake.: Chemical Characterization and Source Apportionment of PM$_{2.5}$ in Rabigh, Saudi Arabia, Aerosol Air Qual Re., 16(12), 3114-3129, 10.4209/aaqr.2015.11.0658, 2016.

Niu, H.W., He, Y.Q., Lu, X.X., Shen, J., Du, J.K., Zhang, T., Pu, T., Xin, H.J., Chang, L.: Chemical composition of precipitation in the Yulong Snow Mountain region, Southwestern China. Atmos. Res. 144, 195-206, https://doi.org/10.1016/j.atmosres.2014.03.010, 2014.

Okuda, T., T. Iwase, H. Ueda, Y. Suda, S. Tanaka, Y. Dokiya, K. Fushimi, and M. Hosoe.: Long-term trend of chemical constituents in precipitation in Tokyo metropolitan area, Japan, from 1990 to 2002, Sci. Total Environ. 339(1), 127-141, https://doi.org/10.1016/j.scitotenv.2004.07.024, 2005.

Wang, W.X., Xu, P.J.: Research Progress in Precipitation Chemistry in China, Progress in Chemistry, Z1, 2009.

Padoan, E., Ajmone-Marsan, F., Querol, X., Amato, F.: An empirical model to predict road dust emissions based on pavement and traffic characteristics, Environ. Pollut. 237, 713-720, https://doi.org/10.1016/j.envpol.2017.10.115, 2017.

Pan, Y. P., Wang, Y. S., Tang, G. Q., Du, W.: Spatial distribution and temporal variations of atmospheric sulfur deposition in Northern China: insights into the potential acidification risks, Atmos. Chem. Phys. 1675-1688, https://doi.org/10.5194/acp-13-1675-2013, 2013.

Prather, K. A., T. H. Bertram, V. H. Grassian, G. B. Deane, M. D. Stokes, P. J. DeMott, L. I. Aluwihare, B. P. Palenik, F. Azam, and J. H. Seinfeld.: Bringing the ocean into the laboratory to probe the chemical complexity of sea spray aerosol, P. Natl. Acad. Sci. USA. 110(19), 7550-7555, https://doi.org/10.1073/pnas.1300262110, 2013.

Pu, W., W. Quan, Z. Ma, X. Shi, X. Zhao, L. Zhang, Z. Wang, and W. Wang.: Long-term trend of chemical composition of atmospheric precipitation at a regional background station in Northern China, Sci. Total

Environ., 580, 1340-1350, https://doi.org/10.1016/j.scitotenv.2016.12.097, 2017.

Qiao, T., M. Zhao, G. Xiu, and J. Yu.: Seasonal variations of water soluble composition (WSOC, Hulis and WSIIs) in PM_1 and its implications on haze pollution in urban Shanghai, China, Atmos. Environ., 123, 306-314, https://doi.org/10.1016/j.atmosenv.2015.03.010, 2015.

Qiao, X., Du, J., Kota, S.H., Ying, Q., Xiao, W.Y., Tang, Y.: Wet deposition of sulfur and nitrogen in Jiuzhaigou National Nature Reserve, Sichuan, China during 2015-2016: Possible effects from regional emission reduction and local tourist activities. 233, 267-277. Environ. Pollut. 233, 267-277, https://doi.org/10.1016/j.envpol.2017.08.041, 2018.

Rao, W., G. Han, H. Tan, and S. Jiang.: Chemical and Sr isotopic compositions of precipitation on the Ordos Desert Plateau, Northwest China, Environ. Earth Sci., 74(7), 5759-5771, 2015.

Ren, D., F. Zhao, S. Dai, J. Zhang, and K. Luo.: Trace Element Geochemical in Coal, edited, Science Press, Beijing, China, 2006.

Russell, K. M., J. N. Galloway, S. A. Macko, J. L. Moody, and J. R. Scudlark.: Sources of nitrogen in wet deposition to the Chesapeake Bay region, Atmos. Environ., 32(14), 2453-2465, https://doi.org/10.1016/S1352-2310(98)00044-2, 1998.

Seinfeld, J. H.: Atmospheric Chemistry and Physics of Air Pollution John Wiley & Sons, Inc., New York, 50-51, 1986.

Shen, Z., J. Sun, J. Cao, L. Zhang, Q. Zhang, Y. Lei, J. Gao, R.-J. Huang, S. Liu, and Y. Huang.: Chemical profiles of urban fugitive dust $PM_{2.5}$ samples in Northern Chinese cities, Sci. Total Environ., 569, 619-626, https://doi.org/10.1016/j.scitotenv.2016.06.156, 2016.

Shi, C.W., Zhao, L.Z., Guo, X.B., Gao, S., Yang, J.P., Li, J.H.: The distribution characteristic and influential factors of background values for elements in Shanxi province, Agro-environmental Protection,

15, 24-28, 1996.

Shi, G.L., Liu, G.R., Peng, X., Wang, Y.N., Tian, Y.Z., Wang, W., Feng, Y.C.: A comparison of multiple combined models for source apportionment, including the PCA/MLR-CMB, UNMIX-CMB and PMF-CMB Models, Aerosol Air Qual. R., 14, 2040-2050, 2014.

Sickles II, J.E., Shadwick, D.S.: Air quality and atmospheric deposition in the eastern US: 20 years of change, Atmos. Chem. Phys., 15, 173-197, https://doi.org/10.5194/acp-15-173-2015, 2015.

Simkin, S. M., E. B. Allen, W. D. Bowman, C. M. Clark, J. Belnap, M. L. Brooks, B. S. Cade, S. L. Collins, L. H. Geiser, and F. S. Gilliam.: Conditional vulnerability of plant diversity to atmospheric nitrogen deposition across the United States, P. Natl. Acad. Sci. USA., 113(15), 4086-4091, https://doi.org/10.1073/pnas.1515241113, 2016.

Singh, A., Agrawal, M.: Acid rain and its ecological consequences. J. Environ. Biol. 29, 15-24, 2008.

Smith, S. J., J. v. Aardenne, Z. Klimont, R. J. Andres, A. Volke, and S. Delgado Arias.: Anthropogenic sulfur dioxide emissions: 1850–2005, Atmos. Chem. Phys., 11(3), 1101-1116, https://doi.org/10.5194/acp-11-1101-2011, 2011.

Song, F., Gao, Y.: Chemical characteristics of precipitation at metropolitan Newark in the US East Coast. Atmos. Environ. 43, 4903-4913, https://doi.org/10.1016/j.atmosenv.2009.07.024, 2009.

Song, H., K. Zhang, S. Piao, and S. Wan.: Spatial and temporal variations of spring dust emissions in northern China over the last 30 years, Atmos. Environ., 126, 117-127, https://doi.org/10.1016/j.atmosenv.2015.11.052, 2016.

Song, Y., Y. Zhang, S. Xie, L. Zeng, M. Zheng, L. G. Salmon, M. Shao, and S. Slanina.: Source apportionment of $PM_{2.5}$ in Beijing by positive matrix factorization, Atmos. Environ., 40(8), 1526-1537, https://doi.org/10.1016/j.atmosenv.2005.10.039, 2006.

Sun, L., L. Li, Z. Chen, J. Wang, and Z. Xiong.: Combined effects of nitrogen deposition and biochar application on emissions of N_2O, CO_2 and NH_3 from agricultural and forest soils, Soil Sci. Plant Nutr., 60(2), 254-265, 2014.

Sun, S.D., Jiang, W., Gao, W.D.: Vehicle emission trends and spatial distribution in Shandong province, China, from 2000 to 2014, Atmos. Environ., 147, 190-199, https://doi.org/10.1016/j.atmosenv.2016.09.065, 2016.

Song, M.-L., Zhang, W., Wang, S.-H.: Inflection point of environmental Kuznets curve in Mainland China. Energy Policy 57, 14-20., 2013.

Song, L., Kuang, F.H., Skiba, U., Zhu, B., Liu, X.J., Levy, P., Dore, A., Fowler, D.: Bulk deposition of organic and inorganic nitrogen in southwest China from 2008 to 2013, Environ. Pollut., 227, 157-166, https://doi.org/10.1016/j.envpol.2017.04.031, 2017.

Tai, A. P., L. J. Mickley, and D. J. Jacob.: Correlations between fine particulate matter ($PM_{2.5}$) and meteorological variables in the United States: Implications for the sensitivity of $PM_{2.5}$ to climate change, Atmos. Environ., 44(32), 3976-3984, https://doi.org/10.1016/j.atmosenv.2010.06.060, 2010.

Tao, J., L. Zhang, R. Zhang, Y. Wu, Z. Zhang, X. Zhang, Y. Tang, J. Cao, and Y. Zhang.: Uncertainty assessment of source attribution of $PM_{2.5}$ and its water-soluble organic carbon content using different biomass burning tracers in positive matrix factorization analysis-A case study in Beijing, China, Sci. Total Environ., 543, 326-335, https://doi.org/10.1016/j.scitotenv.2015.11.057, 2016.

Teinilä, K., A. Frey, R. Hillamo, H. C. Tülp, and R. Weller.: A study of the sea-salt chemistry using size-segregated aerosol measurements at coastal Antarctic station Neumayer, Atmos. Environ., 96, 11-19, https://doi.org/10.1016/j.atmosenv.2014.07.025, 2014.

Teng, X., Q. Hu, L. Zhang, J. Qi, J. Shi, H. Xie, H. Gao, and X. Yao.: Identification of major sources of

atmospheric NH3 in an urban environment in northern China during wintertime, Environ. Sci. Technol., 51, 6839−6848, 10.1021/acs.est.7b00328, 2017.

Tian, H., J. Gao, L. Lu, D. Zhao, K. Cheng, and P. Qiu.: Temporal trends and spatial variation characteristics of hazardous air pollutant emission inventory from municipal solid waste incineration in China, Environ. Sci. Technol., 46(18), 10364-10371, 10.1021/es302343s, 2012.

Tian, H., K. Liu, J. Hao, Y. Wang, J. Gao, P. Qiu, and C. Zhu.: Nitrogen oxides emissions from thermal power plants in China: Current status and future predictions, Environ. Sci. Technol., 47(19), 11350-11357, 10.1021/es402202d, 2013.

Tian, H., K. Liu, J. Zhou, L. Lu, J. Hao, P. Qiu, J. Gao, C. Zhu, K. Wang, and S. Hua.: Atmospheric Emission Inventory of Hazardous Trace Elements from China's Coal-Fired Power Plants Temporal Trends and Spatial Variation Characteristics, Environ. Sci. Technol., 48(6), 3575-3582, 10.1021/es404730j, 2014.

Turekian, K. K.: Oceans, Prentice-Hall, New Jersey, United States, 1968.

Tsai, Y.I., Hsieh, L.Y., Kuo, S.C., Chen, C.L., Wu, P.L.: Seasonal and rainfall-type variations in inorganic ions and dicarboxylic acids and acidity of wet deposition samples collected from subtropical East Asia. Atmos. Environ. 45, 3535-3547, https://doi.org/10.1016/j.atmosenv.2011.04.001, 2011.

Vašát, R., L. Pavlů, L. Borůvka, V. Tejnecký, and A. Nikodem.: Modelling the impact of acid deposition on forest soils in north Bohemian Mountains with two dynamic models: The Very Simple Dynamic Model (VSD) and the Model of Acidification of Groundwater in Catchments (MAGIC), Soil Water Res., 10(1), 10-18, 2015.

Velthof, G., J. Lesschen, J. Webb, S. Pietrzak, Z. Miatkowski, M. Pinto, J. Kros, and O. Oenema.: The impact of the Nitrates Directive on nitrogen emissions from agriculture in the EU-27 during 2000-2008,

Sci. Total Environ., 468, 1225-1233, https://doi.org/10.1016/j.scitotenv.2013.04.058, 2014.

Wang, F.Y., Liu, R.J., Lin, X.G., Zhou, J.M.: Arbuscular mycorrhizal status of wild plants in saline-alkaline soils of the Yellow River Delta. Mycorrhiza 14, 133-137, 2004.

Wang, H., J. An, M. Cheng, L. Shen, B. Zhu, Y. Li, Y. Wang, Q. Duan, A. Sullivan, and L. Xia.: One year online measurements of water-soluble ions at the industrially polluted town of Nanjing, China: Sources, seasonal and diurnal variations, Chemosphere, 148, 526-536, https://doi.org/10.1016/j.chemosphere.2016.01.066, 2016a.

Wang, J., Qiu, Y., He, S.T., Liu, N., Xiao, C.Y., Liu, L.X.: Investigating the driving forces of NOx generation from energy consumption in China. Atmos. Chem. Physics., 184, 836-846, 2018.

Wang, K., H. Tian, S. Hua, C. Zhu, J. Gao, Y. Xue, J. Hao, Y. Wang, and J. Zhou.: A comprehensive emission inventory of multiple air pollutants from iron and steel industry in China: temporal trends and spatial variation characteristics, Sci. Total Environ., 559, 7-14, https://doi.org/10.1016/j.scitotenv.2016.03.125, 2016b.

Wang, S., K. Luo, X. Wang, and Y. Sun (2016c), Estimate of sulfur, arsenic, mercury, fluorine emissions due to spontaneous combustion of coal gangue: An important part of Chinese emission inventories, Environ. Pollut., 209, https://doi.org/10.1016/j.envpol.2015.11.026, 107-113.

Wang, Y., R. Wang, J. Ming, G. Liu, T. Chen, X. Liu, H. Liu, Y. Zhen, and G. Cheng (2016d), Effects of dust storm events on weekly clinic visits related to pulmonary tuberculosis disease in Minqin, China, Atmos. Environ., 127, https://doi.org/10.1016/j.atmosenv.2015.12.041, 205-212.

Wang, Q.: Effects of urbanisation on energy consumption in China, Energ. Policy, 65, 332-339, 2014.

Wang, Q., G. Zhuang, K. Huang, T. Liu, C. Deng, J. Xu, Y. Lin, Z. Guo, Y. Chen, and Q. Fu.: Probing the severe haze pollution in three typical regions of China: Characteristics, sources and regional impacts,

Atmos. Environ., 120, 76-88, https://doi.org/10.1016/j.atmosenv.2015.08.076, 2015a.

Wang, X., W. Pu, J. Shi, J. Bi, T. Zhou, X. Zhang, and Y. Ren.: A comparison of the physical and optical properties of anthropogenic air pollutants and mineral dust over Northwest China, Acta Meteorol Sin., 29(2), 180-200, 2015b.

Wang, Y., Y. Xue, H. Tian, J. Gao, Y. Chen, C. Zhu, H. Liu, K. Wang, S. Hua, and S. Liu.: Effectiveness of temporary control measures for lowering $PM_{2.5}$ pollution in Beijing and the implications, Atmos. Environ., 157, 75-83, https://doi.org/10.1016/j.atmosenv.2017.03.017, 2017.

Wei, F. S., Chen, J. S., Wu, Y. Y., Zheng, C.J.: The study of background value in soil across China. Environ. Sci., 12, 12-20, 1991 (in Chinese).

Wei, F.S., Yang, G.Z., Jiang, D.Z., Liu, Z.H., Sun, B.M.: The basic statistics and characteristics of soil elements in China. Environ. Moni. China., 7, 1-6, 1991 (in Chinese).

Wu, J., Li, P., Qian, H., Duan, Z., Zhang, X.: Using correlation and multivariate statistical analysis to identify hydrogeochemical processes affecting the major ion chemistry of waters: a case study in Laoheba phosphorite mine in Sichuan, China, Arab. J. Geosci., 7, 3973–3982, 2014.

Wu, Q., and G. Han.: Sulfur isotope and chemical composition of the precipitation at the Three Gorges Reservoir, Atmos. Res., 155, 130-140, https://doi.org/10.1016/j.atmosres.2014.11.020, 2015.

Wu, J., G. Liang, D. Hui, Q. Deng, X. Xiong, Q. Qiu, J. Liu, G. Chu, G. Zhou, and D. Zhang.: Prolonged acid rain facilitates soil organic carbon accumulation in a mature forest in Southern China, Sci. Total Environ., 544, 94-102, https://doi.org/10.1016/j.scitotenv.2015.11.025, 2016a.

Wu, X.M., Wu, Y., Zhang, S.J., Liu, H., Fu, L.X., Hao, J.M.: Assessment of vehicle emission programs in China during 1998-2013: achievement, challenges and implications, Environ. Pollut., 214, 556-567, https://doi.org/10.1016/j.envpol.2016.04.042, 2016b.

Xiao, H.W., H.-Y. Xiao, A.-M. Long, Y.-L. Wang, and C.-Q. Liu.: Sources and meteorological factors that control seasonal variation of δ ^{34}S values in precipitation, Atmos. Res., 149, 154-165, https://doi.org/10.1016/j.atmosres.2014.06.003, 2014.

Xing, J., J. Song, H. Yuan, X. Li, N. Li, L. Duan, X. Kang, and Q. Wang.: Fluxes, seasonal patterns and sources of various nutrient species (nitrogen, phosphorus and silicon) in atmospheric wet deposition and their ecological effects on Jiaozhou Bay, North China, Sci. Total Environ., 576, 617-627, https://doi.org/10.1016/j.scitotenv.2016.10.134, 2017.

Xu, P., Y. Liao, Y. Lin, C. Zhao, C. Yan, M. Cao, G. Wang, and S. Luan.: High-resolution inventory of ammonia emissions from agricultural fertilizer in China from 1978 to 2008, Atmos. Chem. Phys., 16(3), 1207-1218, https://doi.org/10.5194/acp-16-1207-2016, 2016.

Xu, W., X. Luo, Y. Pan, L. Zhang, A. Tang, J. Shen, Y. Zhang, K. Li, Q. Wu, and D. Yang.: Quantifying atmospheric nitrogen deposition through a nationwide monitoring network across China, Atmos. Chem. Phys., 15(21), 12345-12360, https://doi.org/10.5194/acp-15-12345-2015, 2015.

Yan, W., E. Mayorga, X. Li, S. P. Seitzinger, and A. Bouwman.: Increasing anthropogenic nitrogen inputs and riverine DIN exports from the Changjiang River basin under changing human pressures, Global Biogeochem. Cy., 24(4), https://doi.org/10.1029/2009GB003575, 2010.

Yang, K., J. Zhu, J. Gu, L. Yu, and Z. Wang.: Changes in soil phosphorus fractions after 9 years of continuous nitrogen addition in a Larix gmelinii plantation, Ann. For. Sci., 72(4), 435-442, 2015.

Yang, X., Shen, S.H., Ying, F., He, Q., Ali, M., Huo, W., Liu, X.C.: Spatial and temporal variations of blowing dust events in the Taklimakan Desert, Theor. Appl. Climato., 125, 669-677, 2016a.

Yang, Y., R. Zhou, Y. Yan, Y. Yu, J. Liu, Z. Du, and D. Wu.: Seasonal variations and size distributions of water-soluble ions of atmospheric particulate matter at Shigatse, Tibetan Plateau, Chemosphere, 145,

560-567, https://doi.org/10.1016/j.chemosphere.2015.11.065, 2016b.

Yang, X., S. Wang, W. Zhang, and J. Yu.: Are the temporal variation and spatial variation of ambient SO_2 concentrations determined by different factors? J. Clean Prod., 167, 824-836, https://doi.org/10.1016/j.jclepro.2017.08.215, 2017.

Yu, H. L., He, N. P., Wang, Q. F., Zhu, J. X., Xu, L., Zhu, Z. L., Yu, G. R.: Wet acid deposition in Chinese natural and agricultural ecosystems: Evidence from national-scale monitoring, J. Geophys. Res. Atmos., 121, 1-11, https://doi.org/10.1002/2015JD024441, 2016.

Yu, H., N. He, Q. Wang, J. Zhu, Y. Gao, Y. Zhang, Y. Jia, and G. Yu.: Development of atmospheric acid deposition in China from the 1990s to the 2010s, Environ. Pollut., 231, 182-190, https://doi.org/10.1016/j.envpol.2017.08.014, 2017a.

Yu, Y., S. Zhao, B. Wang, P. Fu, and J. He.: Pollution Characteristics Revealed by Size Distribution Properties of Aerosol Particles at Urban and Suburban Sites, Northwest China, Aerosol Air Qual Re., 17(7), 1784-1797, 10.4209/aaqr.2016.07.0330, 2017b.

Zhai, P.M., Li, X.Y.: On climate background of duststorms over northern China, Acta Geographica Sinica, 58, 2003 (in Chinese).

Zhan, Y., Luo, Y.Z., Deng, X.F., Zhang, K.S., Zhang, M.H., Grieneisen, M.L., Di, B.F., 2018. Satellited-based estimates of daily NO_2 exposure in China using hybrid random forest and spatiotemporal Kriging model. Environ. Sci. Tech. 52, 4180-4189, 2018.

Zhang, S.L., Yang, G.Y.: Changes of background values of inorganic elements in soils of gunagdong province, Soils, 1009-1014, 2012 (in Chinese).

Zhang, T., J. Cao, X. Tie, Z. Shen, S. Liu, H. Ding, Y. Han, G. Wang, K. Ho, and J. Qiang.: Water-soluble ions in atmospheric aerosols measured in Xi'an, China: seasonal variations and sources, Atmos Res.,

102(1), 110-119, https://doi.org/10.1016/j.atmosres.2011.06.014, 2011.

Zhang, X.-X., B. Sharratt, X. Chen, Z.-F. Wang, L.-Y. Liu, Y.-H. Guo, J. Li, H.-S. Chen, and W.-Y. Yang.: Dust deposition and ambient PM_{10} concentration in northwest China: spatial and temporal variability, Atmos. Chem. Phys., 17(3), 1699-1711, https://doi.org/10.5194/acp-17-1699-2017, 2017a.

Zhang, Y., J. Wei, A. Tang, A. Zheng, Z. Shao, and X. Liu.: Chemical Characteristics of $PM_{2.5}$ during 2015 Spring Festival in Beijing, China, Aerosol Air Qual. Re., 17(5), 1169-1180, 10.4209/aaqr.2016.08.0338, 2017b.

Zhang, Z., J. Gao, L. Zhang, H. Wang, J. Tao, X. Qiu, F. Chai, Y. Li, and S. Wang.: Observations of biomass burning tracers in $PM_{2.5}$ at two megacities in North China during 2014 APEC summit, Atmos. Environ., 169, 54-64, https://doi.org/10.1016/j.atmosenv.2017.09.011, 2017c.

Zhang, X., F. Chai, S. Wang, X. Sun, and M. Han.: Research progress of acid precipitation in China, Res. Environ. Sci., 23(5), 527-532, 2010 (in Chinese).

Zhang, Y.Y., Liu, J.F., Mu, Y.J., Pei, S.W., Lun, X.X., Chai, F.H.: Emissions of nitrous oxide, nitrogen oxides and ammonia from a maize field in the North China Plain, Atmos. Environ., 45, 2956-2961, https://doi.org/10.1016/j.atmosenv.2010.10.052, 2011.

Zhang, Y., W. Huang, T. Cai, D. Fang, Y. Wang, J. Song, M. Hu, and Y. Zhang.: Concentrations and chemical compositions of fine particles ($PM_{2.5}$) during haze and non-haze days in Beijing, Atmos. Res., 174, 62-69, https://doi.org/10.1016/j.atmosres.2016.02.003, 2016.

Zhao, C., and K. Luo.: Sulfur, arsenic, fluorine and mercury emissions resulting from coal-washing byproducts: A critical component of China's emission inventory, Atmos. Environ., 152, 270-278, https://doi.org/10.1016/j.atmosenv.2016.12.001, 2017.

Zhao, J., F. Zhang, Y. Xu, and J. Chen.: Characterization of water-soluble inorganic ions in size-

segregated aerosols in coastal city, Xiamen, Atmos. Res., 99(3), 546-562, https://doi.org/10.1016/j.atmosres.2010.12.017, 2011.

Zhao, M., S. Wang, J. Tan, Y. Hua, D. Wu, and J. Hao.: Variation of urban atmospheric ammonia pollution and its relation with $PM_{2.5}$ chemical property in winter of Beijing, China, Aerosol Air Qual. Res., 16(6), 1378-1389, 10.4209/aaqr.2015.12.0699, 2016.

Zheng, B., H. Huo, Q. Zhang, Z. Yao, X. Wang, X. Yang, H. Liu, and K. He.: High-resolution mapping of vehicle emissions in China in 2008, Atmos. Chem. Phys., 9787, https://doi.org/10.5194/acp-14-9787-2014, 2014.

Zhou, Y., Y. Zhao, P. Mao, Q. Zhang, J. Zhang, L. Qiu, and Y. Yang.: Development of a high-resolution emission inventory and its evaluation and application through air quality modeling for Jiangsu Province, China, Atmos. Chem. Phys., 17(1), 211-233, https://doi.org/10.5194/acp-17-211-2017, 2017a.

Zhou, Y., Xing, X.F., Lang, J.L., Chen, D.S., Cheng, S.Y., Wei, L., Wei, X., Liu, C.: A comprehensive biomass burning emission inventory with highspatial and temporal resolution in China, Atmos. Chem. Phys., 17, 2839-2864, https://doi.org/10.5194/acp-17-2839-2017, 2017b.

Figure and table caption

Fig. 1 The spatial distribution of 320 cities and five ecological regions.

Fig. 2 The inter-annual and seasonal variation of pH and EC of the precipitation in China.

Fig. 3 The spatial distribution of pH and EC of the precipitation in China.

Fig. 4 The temporal variation of water-soluble ions in the precipitation.

Fig. 5 The spatial variation of NO_3^-, NH_4^+, and SO_4^{2-} in the precipitation.

Fig. 6 The spatial distribution of Ca^{2+}, Cl^-, F^-, K^+, Mg^{2+}, and Na^+ in the precipitation.

Fig. 7 The triangular diagrams of NF for main alkaline ions.

Fig. 8 The EF_{sea} and EF_{soil} of NO_3^-, SO_4^{2-}, and NH_4^+.

Fig. 9 The spatial variation of SSF, CF, and AF for NO_3^-, NH_4^+, and SO_4^{2-} in the precipitation.

Fig. 10 The seasonal difference of contribution ratios of anthropogenic source, crustal source, and, sea source.

Fig. 11 The local regression coefficient of influential factors for the NO_3^-, NH_4^+, and SO_4^{2-}.

Tab. 1 The comparison of physicochemical properties and chemical composition in the precipitation.

Tab. 2 The mean enrichment factor relative to sea and soil, and the source contribution (%) of major ions in China (SSF denotes sea salt fraction, CF represents the crustal source, AF indicates the anthropogenic fraction).

Tab. 3 The loading matrix of precipitation in four seasons of China.

Tab. 4 The results of stepwise regression method.

Fig. 1
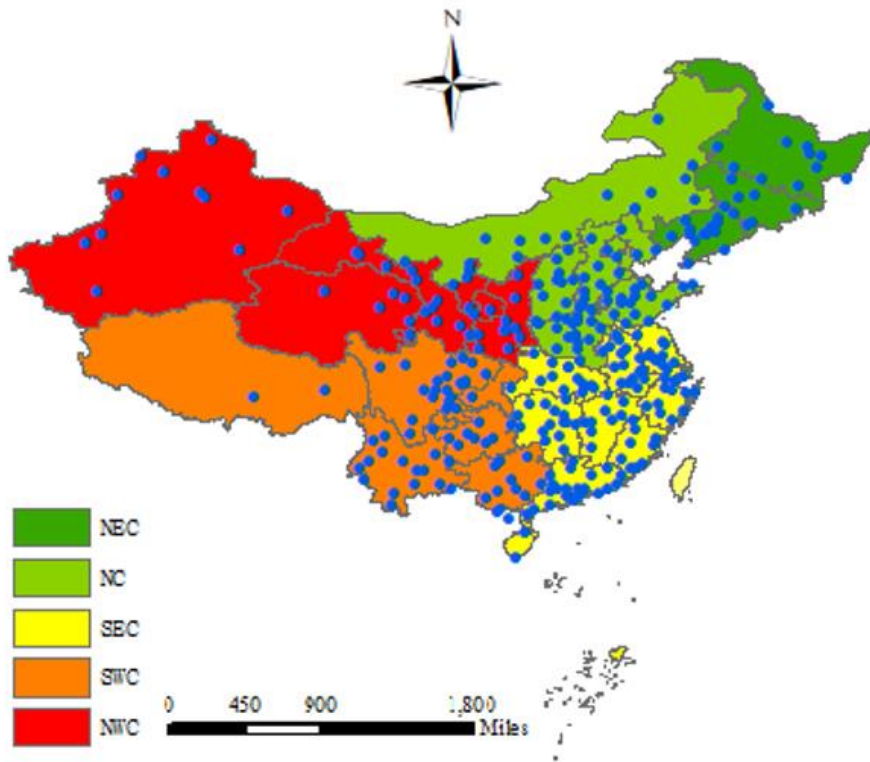
Fig. 2
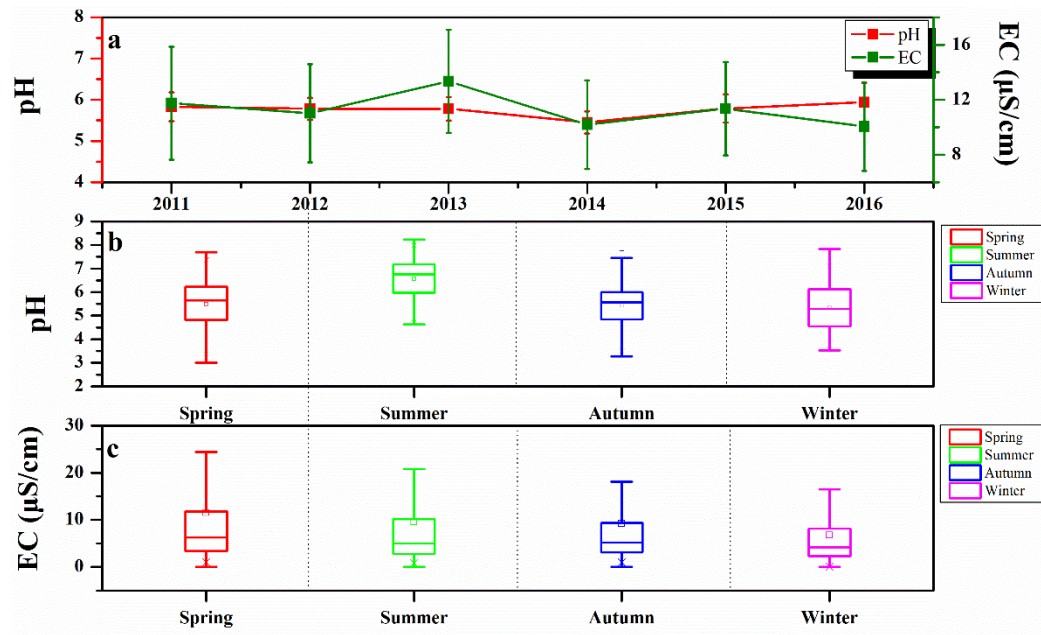
Fig. 3
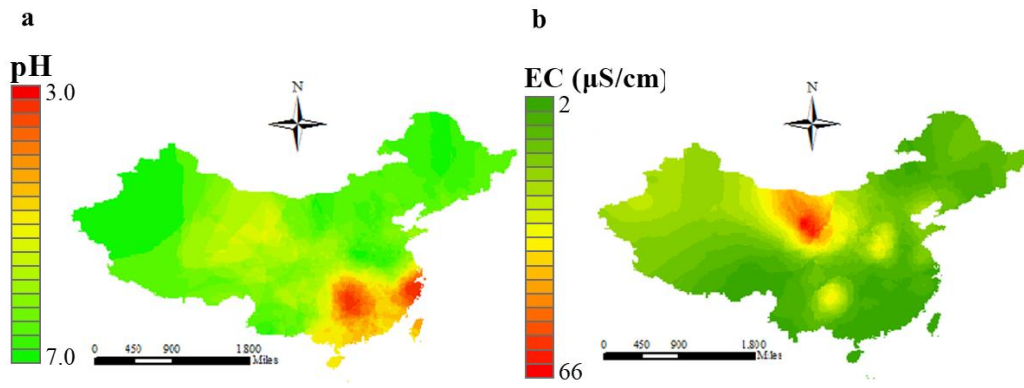
Fig. 4
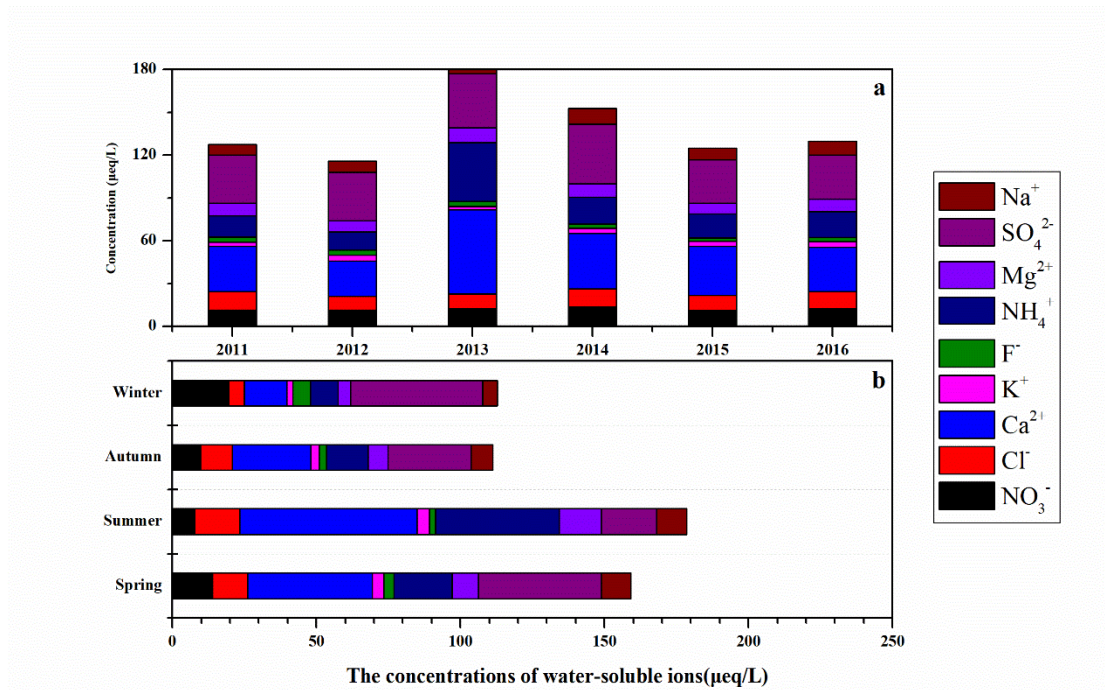
Fig. 5
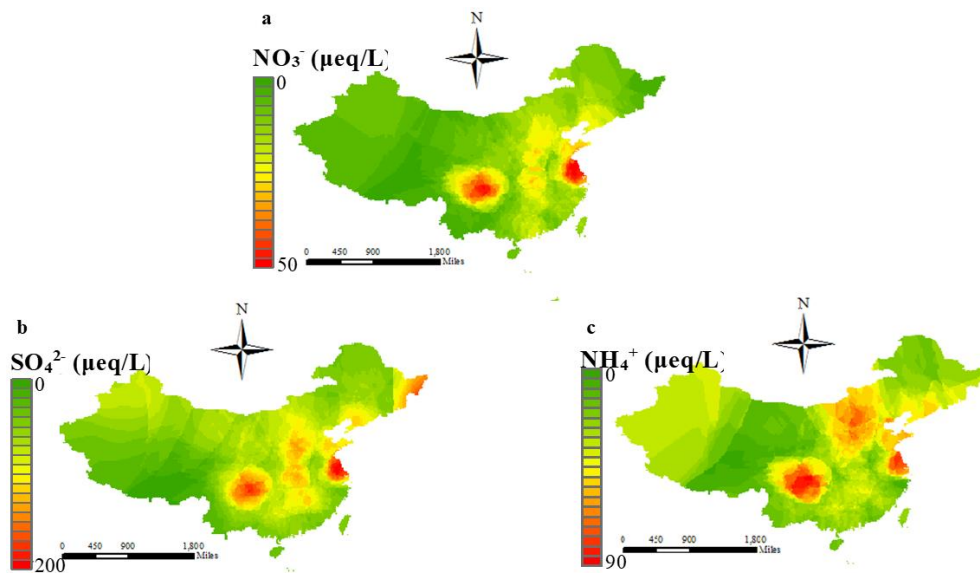
Fig. 6
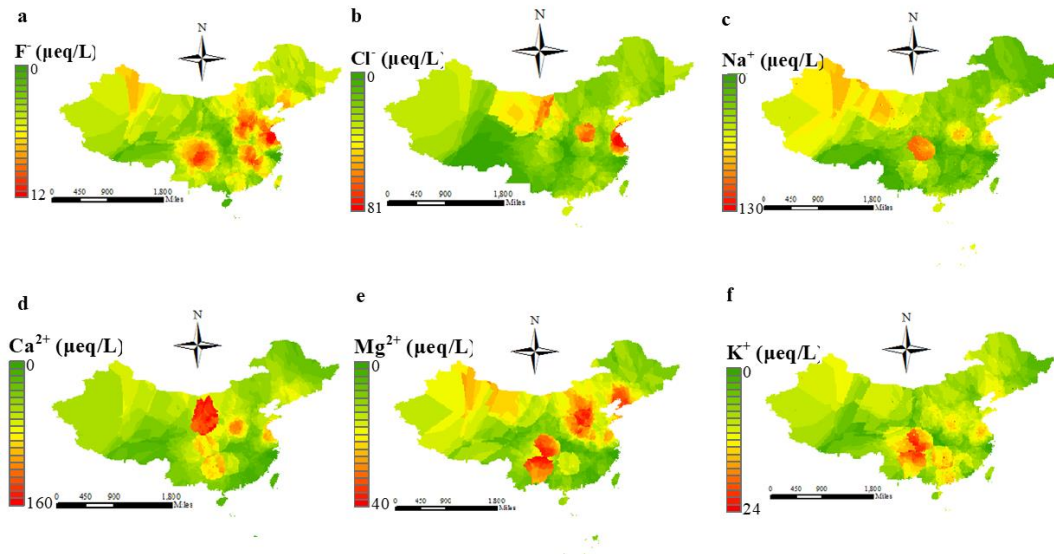
Fig. 7
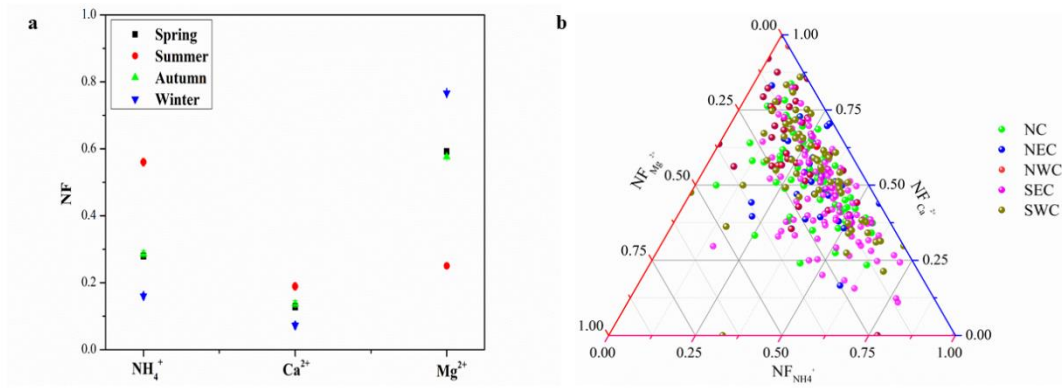
Fig. 8
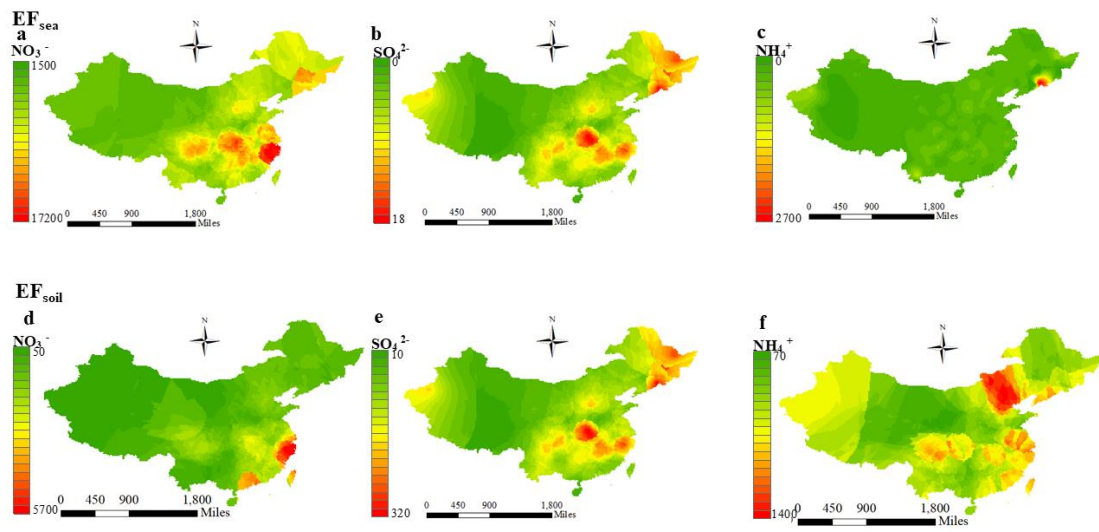
Fig. 9
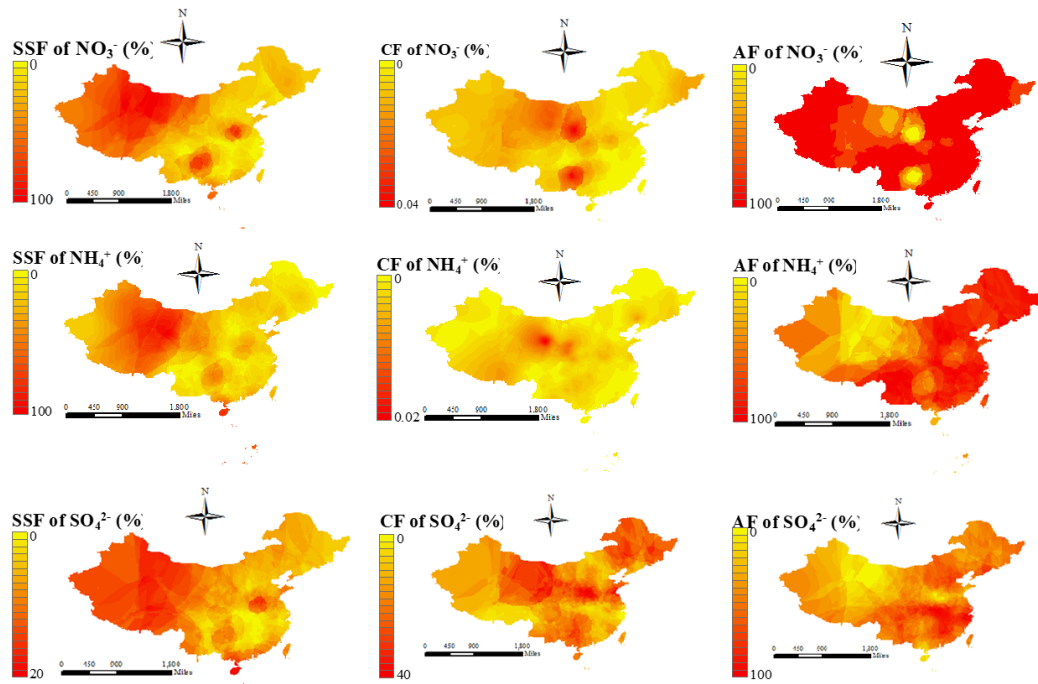
Fig. 10
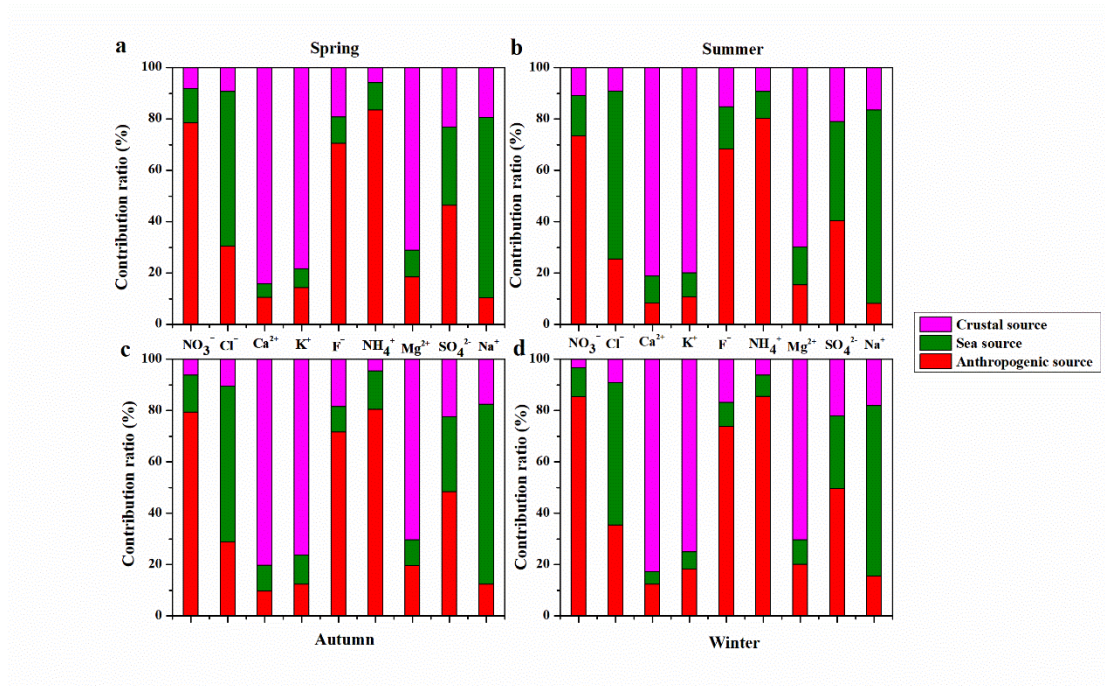
Fig. 11
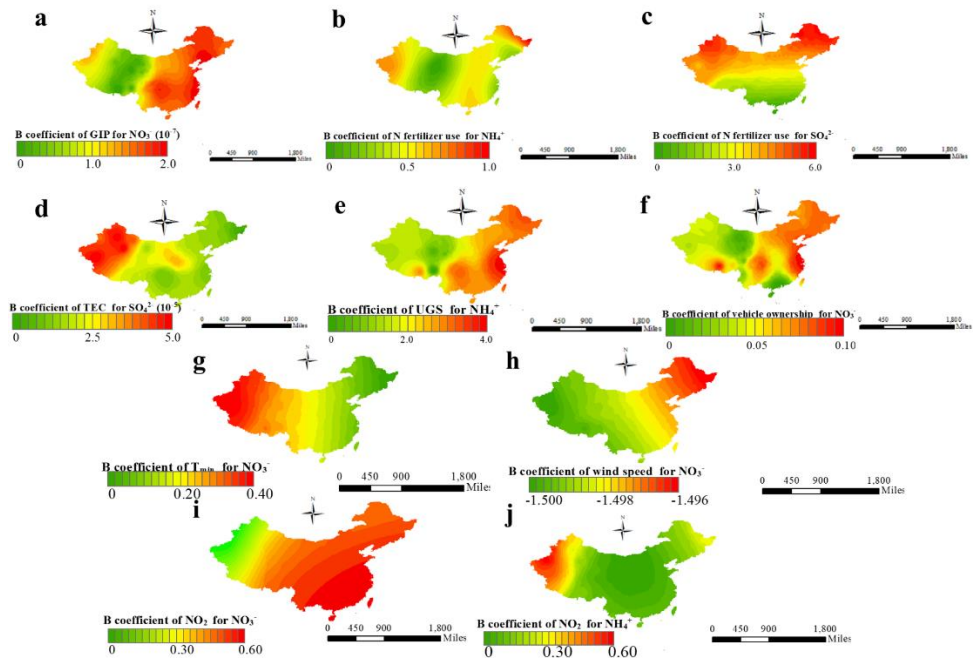
Tab. 1

	pH	EC	NO$_3^-$	Cl$^-$	Ca^{2+}	K$^+$	F	NH$_4^+$	Mg^{2+}	SO$_4^{2-}$	Na$^+$	Year	References
Beijing	5.68	9.89	15.13	6.62	26.27	1.80	2.24	45.33	5.51	31.28	3.39	2011-	This study
Zhengzhou	6.09	26.44	37.10	72.45	109.23	8.25	5.80	23.82	20.54	25.80	6.40	2011-	This study
Harbin	6.13	7.41	9.87	20.71	21.98	5.02	5.03	11.96	9.55	28.76	22.00	2011-	This study
Shenyang	5.76	8.40	24.52	15.90	75.32	2.59	4.32	40.68	22.68	57.57	16.88	2011-	This study
Qingdao	5.32	16.53	5.25	5.79	28.18	2.07	1.34	9.28	9.80	10.96	25.30	2011-	This study
Shanghai	4.39	2.50	40.06	4.15	19.09	1.07	1.45	17.48	4.71	29.13	20.36	2011-	This study
Wuhan	4.68	2.66	11.61	2.12	13.55	0.76	1.07	9.38	2.63	27.93	1.28	2011-	This study
Guangzhou	4.98	2.84	26.74	19.38	41.60	9.42	3.93	13.58	8.33	35.76	9.57	2011-	This study
Chengdu	4.89	6.03	48.08	22.13	44.42	12.60	9.21	65.19	8.23	77.16	15.06	2011-	This study
Lhasa	5.21	4.51	0.50	1.65	7.66	0.48	0.94	0.91	1.28	1.44	1.62	2011-	This study
Urumqi	6.13	13.41	16.87	30.38	115.24	4.76	2.02	73.76	19.41	56.76	28.87	2011-	This study
Lanzhou	5.05	58.06	16.19	4.93	51.84	1.24	1.57	3.05	8.17	33.30	10.87	2011-	This study
Jiuzhaigou	5.95	15.70	9.10	44.10	55.80	34.80	0.86	18.40	5.60	15.90	12.60	2015-	Qiao et al. (2018)
Yulong	5.94	10.30	4.00	1.96	37.7	2.46	1.20	13.20	5.68	28.30	3.72	2012	Niu et al. (2014)
Nam Co	6.59	19.70	10.00	19.20	301	14.50	-	18.10	7.43	15.50	15.40	2005	Li et al. (2007)
Southern	-	-	20.97	31.06	46.68	11.14	-	58.57	22.55	45.97	56.41	2005-	Tsai et al. (2011)
Petra,	6.80	160	35.70	80.60	163.10	26.30	-	18.40	62.30	53.20	75.60	2002-	Al-Khashman et al. (2005)
Tokyo,	4.52	-	30.50	55.20	24.90	2.90	-	40.4	11.5	50.2	37.0	1990-	Okuda et al. (2005)
Guaíba,	5.92	10.8	4.00	13.80	21.50	5.81	5.90	38.90	8.85	23.10	15.10	2002	Migliavacca et al. (2005)
Sao Paulo,	-	-	15.60	0.90	5.50	3.70	-	27.90	1.70	8.60	3.60	2000	Fornaro and Gutz (2003).
Singapore	-	-	16.80	22.10	21.7	3.96	-	17.3	7.46	58.7	31.1	1997-	Balasubramanian et al. (2001)
Newark,	-	-	14.40	10.70	6.00	1.30	-	24.40	3.30	38.10	10.90	2006-	Song and Gao (2009)
Patras,	5.16	--	19.40	114.30	98.50	6.60	--	16.30	30.40	46.10	90.20	2000-	Glavas and Moschonas (2002)
Sardinia,	5.18	--	29	322	70	17	--	25	77	90	252	1992-	Le Bolloch and Guerzoni (1995)
Adirondack,	4.50	--	22.60	2.14	3.59	0.33	--	10.50	0.99	36.90	1.61	1988-	Ito et al. (2002)

Tab. 2

	EF_{sea}	EF_{soil}	SSF	CF	AF
NO_3^-	3507.49	59.36	0	0.02	99.98
Cl^-	1.13	169.88	88.31	0.59	11.10
Ca^{2+}	231.56	1.00	0.06	99.94	0
K^+	16.16	0.83	4.88	95.12	0
F^-	5864.28	9.96	0.02	10.04	89.94
NH_4^+	10.51	86.31	0.10	0.01	99.89
Mg^{2+}	10.18	0.55	2.94	97.06	0
SO_4^{2-}	7.22	5.13	13.85	19.50	66.65
Na^+	1.00	1.83	64.66	35.34	0

Tab. 3

Season	Variable	F1	F2	F3
Overall	NO_3^-	**0.71**	0.24	0.45
	Cl^-	0.43	**0.64**	-0.12
	Ca^{2+}	0.42	-0.22	**0.75**
	K^+	0.39	0.18	**0.72**
	F^-	**0.68**	-0.20	0.45
	NH_4^+	**0.74**	0.35	0.13
	Mg^{2+}	-0.41	0.10	**0.66**
	SO_4^{2-}	**0.63**	0.23	0.14
	Na^+	-0.02	**0.65**	0.45
Spring	NO_3^-	**0.76**	0.11	-0.32
	Cl^-	-0.33	**0.59**	0.26
	Ca^{2+}	0.32	-0.16	**0.80**
	K^+	-0.36	0.06	**0.78**
	F^-	**0.70**	-0.10	0.20
	NH_4^+	**0.68**	0.29	-0.46
	Mg^{2+}	-0.38	0.42	**0.69**
	SO_4^{2-}	**0.77**	0.31	0.22
	Na^+	-0.04	**0.72**	0.46
Summer	NO_3^-	**0.63**	0.24	-0.33
	Cl^-	0.42	**0.66**	-0.38
	Ca^{2+}	0.44	-0.26	**0.85**
	K^+	-0.37	0.19	**0.70**
	F^-	**0.54**	-0.32	0.48
	NH_4^+	**0.59**	0.33	-0.47
	Mg^{2+}	0.32	-0.38	**0.60**
	SO_4^{2-}	**0.56**	0.36	0.34
	Na^+	-0.09	**0.75**	0.49
Autumn	NO_3^-	**0.73**	-0.14	0.38
	Cl^-	-0.39	**0.62**	0.29
	Ca^{2+}	0.32	-0.16	**0.80**
	K^+	0.45	-0.09	**0.68**
	F^-	**0.68**	-0.15	0.28

	NH$_4^+$	**0.69**	0.42	-0.45
	Mg^{2+}	-0.29	0.32	**0.71**
	SO$_4^{2-}$	**0.68**	-0.29	0.23
	Na$^+$	-0.14	**0.69**	-0.37
Winter	NO$_3^-$	**0.79**	0.23	-0.36
	Cl$^-$	-0.38	**0.49**	0.29
	Ca^{2+}	0.39	-0.35	**0.65**
	K$^+$	-0.39	0.08	**0.72**
	F$^-$	**0.75**	0.08	-0.24
	NH$_4^+$	**0.73**	0.26	-0.42
	Mg^{2+}	0.35	-0.49	**0.75**
	SO$_4^{2-}$	**0.79**	0.22	0.36
	Na$^+$	-0.16	**0.54**	0.33

Tab. 4

Dependent variables	Independent variables	Partial regression coefficients	R^2	t value	p value
NO_3^-	GIP	8.42×10^{-8}	0.62	4.03	0.00
	Vehicle ownership	0.03		-2.39	0.01
	NO_2	0.34		4.29	0.00
	T_{min}	0.15		1.34	0.02
	Wind speed	-1.49		-1.69	0.03
Cl^-	Dust days	0.12	0.52	2.14	0.04
Ca^{2+}	PM_{10}	0.36	0.56	3.26	0.00
	Dust days	132.74		2.99	0.00
K^+	Dust days	2.09	0.49	2.03	0.02
F^-	GIP	0.54×10^{-7}	0.50	2.31	0.02
NH_4^+	N fertilizer use	0.14	0.48	2.46	0.02
	UGS	1.33×10^{-4}		1.79	0.04
	NO_2	0.25		1.98	0.03
Mg^{2+}	Dust days	2.36	0.43	1.65	0.05
SO_4^{2-}	TEC	2.80×10^{-5}	0.64	3.07	0.00
	N fertilizer use	3.36		3.59	0.00
Na^+	Dust days	2.46	0.46	1.69	0.04